7-2022

Influence of Paclitaxel Nanomedicine on the Pancreatic Tumor Immune Components

Godwin Peasah-Darkwah
The University of Texas Rio Grande Valley

INFLUENCE OF PACLITAXEL NANOMEDICINE ON THE PANCREATIC TUMOR IMMUNE COMPONENTS

A Thesis

by

GODWIN PEASAH-DARKWAH

Submitted in Partial Fulfillment of the

Requirements for the Degree of

MASTER OF SCIENCE

Major Subject: Biochemistry and Molecular Biology

The University of Texas Rio Grande Valley

July 2022

INFLUENCE OF PACLITAXEL NANOMEDICINE ON THE PANCREATIC TUMOR IMMUNE COMPONENTS

A Thesis
by
GODWIN PEASAH-DARKWAH

COMMITTEE MEMBERS

Dr. Subhash Chauhan
Chair of Committee

Dr. Bilal Bin Hafeez
Committee Member

Dr. Murali Yallapu
Committee Member

Dr. Nirakar Sahoo
Committee Member

July 2022

ABSTRACT

Peasah-Darkwah, Godwin, Influence of Paclitaxel Nanomedicine on the Pancreatic Tumor Immune Components. Master of Science (MS), July, 2022, 97 pp., 27 figures, references, 136 titles.

Pancreatic cancer (PanCa) is one of the leading causes of cancer-related mortalities in the U.S due to ineffective therapeutic options. Pancreatic tumors are highly desmoplastic and inhibit efficient uptake of therapeutic payloads. Paclitaxel (PTX) has been tested in PanCa therapy with marginally better clinical outcomes, but remain limited by its poor hemocompatibility, biodistribution and intracellular accumulation in tumor cells. Thus, we synthesized a next-generation nanoparticle system for PTX to improve its pharmacokinetics and pharmacodynamics (PKPD) in treating PanCa. We also examined ability of the nano formulation to potentiate gemcitabine (GEM) activity in combating chemoresistance in the pancreatic tumor microenvironment (TME).We generated a multi-layered Pluronic F127 coated paclitaxel loaded poly(lactic-co-glycolic acid) nanoparticle formulation (PPNPs) which demonstrated superior therapeutic efficacy over free PTX, effectively potentiated GEM activity in the pancreatic TME, and efficiently reprogrammed oncogenic M2 macrophages to an M1 profile to maintain a pro-inflammatory phenotype.

DEDICATION

I dedicate this thesis to God Almighty who has been my ever-present help and source of strength, and to my family and friends who have supported me throughout this journey.

ACKNOWLEDGMENTS

I will always be grateful to Dr. Subhash Chauhan, chair of my dissertation committee, for all his mentoring and advice. From research design, project execution and data analysis, to manuscript editing, he encouraged me to complete this process through his infinite patience and guidance. Special thanks go to my immediate mentor, Dr. Vivek Kashyap, who practically held my hand through it all and helped me complete this project, and to my dissertation committee members: Dr. Murali Mohan Yallapu, Dr. Bilal Bin Hafeez and Dr. Nirakar Sahoo. Their advice, input, and comments on my thesis helped to ensure the quality of my intellectual work.

I would also like to thank my colleagues at the University of Texas Rio Grande Valley Biomedical Research Facility who helped me acquire reagents for my research. Also, I would like to acknowledge my family and friends for their constant support and pieces of advice as I wrote this manuscript.

TABLE OF CONTENTS

Page

LIST OF FIGURES

Page

CHAPTER I

INTRODUCTION

Pancreatic cancer (PanCa) has been classed as the fourth leading cause of cancer-associated deaths in the United States (US) alone (Sung et al.). This is mostly as a result of difficulty in detection of the disease, as well as development of chemoresistance mediated by the immunosuppressive tumor microenvironment (TME) (Ankeny et al.). According to Hoff et al. (2013), combination of Gemcitabine (GEM) and Abraxane® (albumin-bound paclitaxel) barely resulted in an approximately 8.5 months increase in overall survival (OS) compared to just 6.7 months for single GEM therapy (Von et al.). Various novel drugs have been churned out in hopes of curing PanCa but with little to no avail because of several reasons such as poor immune tolerance, increased toxicity, poor bioavailability and distribution and rapid renal clearance (Di Marco et al.; Kleynberg, Sofi and Chaudhary; Pedersen; Rapoport et al.). These drugs or combination therapies thereby invariably fail by Phase II or Phase III clinical studies resulting in massive financial losses. Typical characteristics of PanCa that lead to these dreadful outcomes include an increasingly tortuous, leaky vasculature (Pries et al.; Provenzano et al.; Triantafyllos Stylianopoulos et al.), highly desmoplastic and hypoxic stroma (Albrecht Neesse et al.), as well as downregulated carrier and transport proteins (Farrell et al.).

These features create an immunosuppressive TME surrounding the tumor that results in inefficient drug delivery and development of chemoresistance as a result of an elevated interstitial fluid pressure (Jain). This inhibits drug delivery through the tumor vasculature to the extracellular environment, and makes PanCa exceptionally difficult to treat (Siegel RL). Stand-alone immunotherapies have rarely yielded significant clinical outcomes, mainly because of the dense, hypoxic pancreatic TME characterized by enormous fibrosis and high desmoplasia that impedes drug therapy (Christine Feig et al.; Sperb, Tsesmelis and Wirth). GEM is the current gold standard for chemotherapeutic drugs used in treating PanCa. However, PDAC tumours have acquired resistance to GEM by downregulating nucleoside transporters that facilitate GEM uptake in these cells and increasing activity of cytidine deaminase that degrades intracellular GEM (Farrell et al.; Frese et al.). This has necessitated development of alternative drugs that can demonstrate efficient anti-cancer activity against PanCa, particularly PDAC. Paclitaxel (PTX) is one such compound that has been utilized in PanCa therapy recently. PTX is a natural anti-cancer agent isolated from Pacific Yew trees and utilized as a second line therapy in treating PanCa (Maeda et al.). PTX has demonstrated potent anti-tumour activity in several cancer types, including PanCa (He et al.). In a recent study, it was demonstrated that Abraxane® enhanced GEM uptake, as PTX downregulated activity of cytidine deaminase and facilitated increased intracellular GEM concentration (Frese et al.). Numerous studies have also demonstrated therapeutic efficacy of PTX in altering TME and desmoplasia to enhance GEM absorption and intracellular localization (Von et al.). However, the main shortcomings of PTX include poor solubility and hemocompatibility (Meng et al.).

To avert this, various researchers have developed nano formulations of PTX to improve its activity. However, off-target delivery is one of the main limitations of current nano formulations of PTX such as Abraxane®. Others include rapid clearance by the renal system thereby decreasing the systemic half-life of PTX, phagocytosis by immune cells and poor drug delivery through the tumour microenvironment directly to tumour cells (Maeda et al.). Herein, we have characterized a novel PLGA-PTX nano formulation (PPNPs) by integrating the hydrogel Pluronic F127 which chemo sensitizes the immune tumour microenvironment to chemotherapy thereby improving efficacy of PTX in PanCa patients. Poly (lactic-co-glycolic-acid) is a biodegradable and hemo-compatible polymer approved for use in drug delivery systems by the U.S. Food and Drugs Administration (FDA) (Dinarvand et al.; Danhier et al.). Pluronic F127 has demonstrated therapeutic benefits in reversing drug resistance in the TME (Sosnik; W. Zhang et al.). Herein, we have shown that PPNPs effectively inhibit PanCa growth and metastasis in PanCa cell lines in a manner that is significantly superior to free PTX, and subsequently chemo sensitizes the pancreatic TME to GEM therapy in vitro.

Statement of the Problem

The pancreatic tumor immune microenvironment components cause a suboptimal delivery of therapeutic agents in tumors that eventually result in development of chemoresistance. The enhanced recruitment of tumor associated fibroblasts (TAFs), pancreatic stellate cells (PSCs), cancer initiating cells (CICs), tumor associated macrophages (TAMs) as well as other immunosuppressive components play a pivotal role in development, progression, metastasis, and therapy resistance of PanCa (Yoshikawa et al.; Mohammed et al.; Haqq et al.; Apte, Pirola and Wilson; Pan et al.). This dense desmoplastic stromal TME impedes drug delivery and contributes to chemoresistance by building high interstitial fluid pressure and downregulating transport proteins leading to poor prognosis and worse outcomes in PanCa patients.

Statement of the Purpose

Targeting malignant pancreatic cells by small molecule inhibitors have demonstrated promising activity in improving immunotherapy in pre-clinical mouse models (Cassetta and Kitamura; Anfray et al.; Li et al.). An approach to navigating the stromal burden in the pancreatic TME and improving patient outcomes has been the development of combination therapies such as GEM combination with taxanes such as docetaxel and PTX (Von Hoff et al.). On September 6, 2013, the U.S Food and Drugs Administration (FDA) consented to the use of combination treatment regimens such as nab-paclitaxel with GEM, and this has moderately ameliorated (~1.8 months) PanCa patient's survival (8.5 months vs. 6.7 months with GEM alone) (Massey et al.). Clinical studies have demonstrated that combination treatments involving PTX augmented the tumor microenvironment and desmoplasia by mechanisms yet to be identified and thereby significantly increased the rate of GEM uptake in pancreatic tumors (Von Hoff et al.).

However, poor water solubility and substandard delivery limits effective long-term accumulation of PTX in pancreatic tumors and overall systemic circulation (Meng et al.). This has necessitated development of novel strategies to improve PTX bioavailability and distribution in circulation and improve patient outcomes. Thus, it is entirely possible that therapeutic outcomes regulated by the application of PTX can be further improved by employing targeted nano formulations of PTX with improved drug delivery outcomes and reversal of drug resistance in the TME. Indeed, a distinctive, Pluronic F127-coated paclitaxel loaded nanoparticles (PPNPs) formulation has been previously generated and it efficiently demonstrated lipid raft mediated internalization, effective growth suppression and metastasis in vitro, and in chemo-naïve and chemo-exposed orthotopic xenograft mouse models (Murali M Yallapu et al.; Murali Mohan Yallapu et al.; Massey et al.; Shetty et al.). These nanoparticles (NPs) also disrupted De Novo Lipid Synthesis in PanCa Cells and enhanced GEM efficacy (Massey et al.; Shetty et al.; Murali M Yallapu et al.; Murali Mohan Yallapu et al.). Based on this compelling evidence, it is hypothesized that PPNPs can not only enhance efficacy of PTX, but also influence components of the pancreatic immune TME and could be a novel therapeutic modality in PanCa chemotherapy to improve tumor immune surveillance and yield positive outcomes in clinical settings. This study would explore two main objectives:

1: To evaluate chemo-sensitization and tumor microenvironment regulation of PPNPs in PanCa cells.

In this study, therapeutic efficacy of PPNPs would be determined by various in vitro (Cell Proliferation, Clonogenic, Boyden Chamber Cell Migration and Boyden Chamber Matrigel Cell

Invasion Assays), and ex vivo (Immunoblotting and Quantitative Real-Time Polymerase Chain Reaction (qRT-PCR)) studies using relevant PanCa cell lines.

Examination of the underlying molecular mechanisms that contribute to the PPNPs mediated inhibition of oncogenic signaling pathways that are involved in developing desmoplastic TME and chemo-resistance using relevant PanCa cells (Panc-1, HPAF-II, AsPC-1 and MIA PaCa-II), would be conducted.

2: To investigate the effects of PPNPs on GEM activity in the pancreatic TME and associated immune components.

This study would interrogate the impact of PPNPs in combination with GEM on key molecules involved in pancreatic desmoplasia using stromal components. The study would also determine how PPNPs suppress polarization of M1 macrophages into Tumor Associated Macrophages (TAMs) and reprogram TAMs into an M1 profile using murine macrophages as a model system in vitro.

.

CHAPTER II

REVIEW OF LITERATURE

Pancreas

The pancreas is an abdominal gland which is roughly six inches long and positioned between the stomach and the spine. Its pear-shaped nature affords a wide surface area to execute bodily functions (Network "What Is the Pancreas?"). This gland is both exocrine and endocrine and carries out two vital functions in the body – digestion and regulation of glucose levels in blood (Network "What Is the Pancreas?"). During food digestion, the exocrine cells secrete digestive enzymes through a system of minor ducts that converge into the main pancreatic duct. The pancreatic duct is responsible for transporting these pancreatic enzymes and other secretions, collectively called pancreatic juice, towards the common bile duct which also transports bile. These two ducts then converge at the ampulla of Vater in the duodenum and the bile and pancreatic enzymes can collectively enter duodenum to facilitate breakdown of fats, proteins, and sugars (Network "What Is the Pancreas?").

Pancreatic Cancer

Pancreatic cancer (PanCa) arises when an abnormality in normal pancreatic cells stimulates excessive proliferation of these cells that eventually results in a malignant tumor (Kleeff et al.).

These abnormalities that drive over proliferation of pancreatic cells usually arise from alterations in genomic sequences because of epigenetic modifications, mutations, or lifestyle changes such as smoking, obesity, drinking and even age (Network "What Is Pancreatic Cancer?"). Exact causes of PanCa are barely understood but almost 10% of PanCa are classified as hereditary. Signs and symptoms of PanCa include jaundice, nausea, pancreatitis and weight loss (Network "What Is Pancreatic Cancer?"). There are two main types of PanCa based on origin of development - exocrine tumors and neuroendocrine tumors. The majority of pancreatic tumors are exocrine, forming about 85% of all pancreatic tumors, and the most common type is pancreatic ductal adenocarcinoma (PDAC) (Massey et al.). Neuroendocrine tumors constitute the remaining percentage of pancreatic tumors, and they are less common. As such, this study focuses on the main type of PanCa – pancreatic ductal adenocarcinoma, henceforth used interchangeably with “PanCa” to represent exocrine pancreatic tumors.

Pancreatic Ductal Adenocarcinoma

Pancreatic ductal adenocarcinoma (PDAC) is a malignant growth of the ductal cells in the small pancreatic duct, often in the head of the pancreas. Due to the narrow diameter of these ducts, malignant growth of these ductal cells blocks normal flow of pancreatic juices and impair proper functioning of the pancreas in the body. PDAC is the most prevalent pancreatic neoplasm and forms about >90% of pancreatic tumor cases (Hezel et al.).

Epidemiology

To ascertain the prevalence of PDAC and co-morbidities, it is imperative to factor the number of PDAC-diagnosed patients, morbidity, and mortality rates (Simoes et al.). A study by GLOBOCAN in 2020 found that the number of new reports of PDAC was 495,773, and this ranked as the fourteenth most prevalent cancer (Ushio et al.).

The number of mortality cases, however, that was secondary to PDAC was 466,003 per year, ranking it seventh as a primary cause of cancer-associated mortality (Sung et al.). The one-year OS rate of PDAC patients is barely 24%, whereas the five-year OS rate is just 9% (Sung et al.). This is, in part, due to an ineffective therapeutic response by current treatment options as well as challenges with early detection of the disease (Massey et al.). New cases of PDAC is highly variable globally, with the most age-standardized incidence rates reported in Europe and North America, while Africa and Central Asia recorded the least age-standardized incidence rates (Sung et al.). Comparison of risk associated with PDAC occurrence between developed regions and less developed areas posted age-standardized incidence rates of about 7.2 and 2.8, respectively, per 100,000; and about >50% of all PanCa cases are diagnosed in more developed areas (Simoes et al.). Males have higher incidence rates of PDAC (5.7 per 100,000, with 262,865 cases) than females (4.1 per 100,000, with 232,908 cases) (Ushio et al.). Moreover, data from the United States SEER program (Surveillance, Epidemiology, and End Results) shows a marginally increased risk of PanCa incidence of PanCa with time (SEER). One major risk factor for PDAC is old age: the age-specific incidence rates of PanCa increased from 10.4 per 100,000 in those aged 55–59, to 24.0 in those aged 65–69, and to 55.7 in those aged 75 and beyond (Simoes et al.). Interestingly, Black/African-Americans recorded the highest percentage of PanCa incidence among all racial and ethnic groups in the United States (U.S), and Black Americans are highly likely to be predisposed to advanced disease with fairly low probability of being eligible for surgical procedure (Yeo). Factors that may influence this health disparity of PanCa observed in Black/African Americans may possibly include racial differences such as metabolism of cigarette smoke, low socio-economic status, and alcohol consumption etc.

Low socio- economic status, in particular, has been linked with advanced stage of PanCa diagnosis with decreased positive rates of adjuvant therapy (Yeo).

Causes and Risk Factors of PDAC

The exact mechanisms that underpin PDAC development and progression is not well and truly understood but it has been postulated that various risk factors such as pancreatitis (Lowenfels et al.), Type II diabetes (Yeo), smoking (Network "What Is Pancreatic Cancer?"), alcoholism, obesity and even age plays a vital role in establishment of PDAC (Figure 2-1) (Yeo). Also, previous studies have highlighted that PDAC development might be hereditary through germline mutations (Network "What Is Pancreatic Cancer?"). This emphasizes the role of lifestyle activities on malignant growth of PanCa cells. Nonetheless, lifestyle activities are somewhat manageable at best to help avert cancer development and progression in subsequent generations through education and awareness on the dangers of epigenetic factors in establishing PDAC. Alterations in DNA sequences that drive PDAC establishment ultimately sets the tone for progression of PDAC, and establishment of a dense, hypoxic desmoplastic stroma that establishes a near-impenetrable TME that impedes conventional therapies targeting PDAC. According to Pelosi et. al., (2017), the four most commonly mutated genes in PDAC include proto-oncogenic Kirsten-Rat sarcoma viral oncogene homolog (K-Ras), and the tumor suppressors, SMAD4, Tumor protein 53 (TP53) and P16/ cyclin-dependent kinase inhibitor 2A (P16/CDKN2A) (Pelosi, Castelli and Testa).

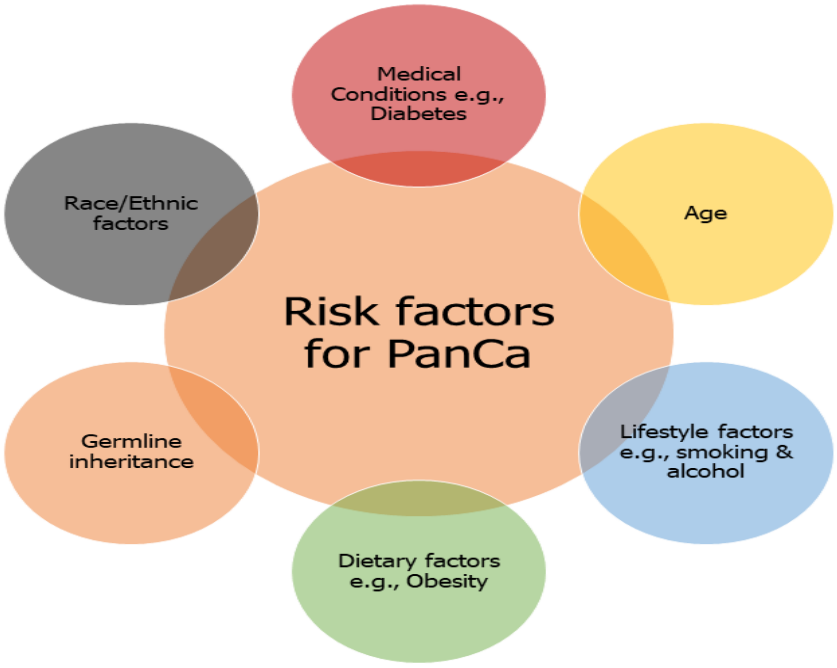

Figure 2-1**.** Various risk factors contribute to the establishment and progression of PanCa. These factors can predispose an individual to acquisition of PanCa.

Signs and Symptoms of PDAC

PDAC is incredibly hard to manage because of the difficulty in detection at an early stage of the disease (Siegel RL). The early stages of the tumor are largely asymptomatic and symptoms begin to manifest only at an advanced stage of the disease (Lindquist et al.). There has been limited research on early detection of the disease, with the protein CA 19-9 having been identified as a potential biomarker. However, the levels of this protein have been shown to not reliably reflect the presence of PanCa (Engle et al.). Even at an advanced stage of the disease, most of the usual symptoms are non-specific such as asthenia, anorexia, weight loss, abdominal pain among others (Keane et al.), and these signs or symptoms can even be misinterpreted for

other diseases such as pancreatitis or ulcer (Rawla, Sunkara and Gaduputi; Freelove and Walling).

Tumor Microenvironment and Immunosuppression in PDAC

PDAC is unique because the intertumoral effector cells are in significantly low numbers, compared to other solid tumors for which there is prominent infiltration of the tumor cells by T lymphocytes (Ino et al.; Fridman et al.). There is also an enormous rate of infiltration of immunosuppressive leukocytes into the TME. Furthermore, during the establishment and progression of PanCa, there is a strong desmoplastic stromal reaction that promotes angiogenesis and aids immune evasion (Ino et al.; Protti and De Monte). Also, the RAS oncogene controls an inflammatory cascade that establishes immune privilege in the TME of PanCa (Collins et al.). This dense stromal reaction, reinforced with platelet-derived growth factor (PDGF), proteoglycans, and fibronectin, creates a seemingly impenetrable wall that interacts with cancer cells and aids in progression and invasion, while at the same time serving as an immune barrier to immune effector cells capable of attacking tumor cells (C. Feig et al.). The increased recruitment of TAFs (Pan et al.), PSCs (Haqq et al.; Apte, Pirola and Wilson), CICs (Mohammed et al.), and TAMs (Yoshikawa et al.) also plays a pivotal role in development, progression, metastasis, and therapy resistance of PanCa. In addition, certain signaling pathways during cancer such as K-Ras (Almoguera et al.), nuclear factor kappa-light-chain-enhancer of activated B cells (NF-κB) (Carbone and Melisi), C-X-C chemokine ligand 12/C-X-C chemokine receptor 4 (CXCL12/CXCR4) (Xu et al.), and Sonic Hedgehog (SHH) (Bailey, Mohr and Hollingsworth; Bailey et al.) have been shown to be crucial in modulating the TME, PDAC development, progression, and metastasis (Borst; Allum).

These elements lead to a suboptimal delivery of therapeutic agents in tumors that eventually results in enhanced chemo-resistance. This uniquely immunosuppressive and highly desmoplastic TME (with pronounced fibrosis and extracellular matrix accumulation) is dominant in most cases of PDAC, and this presents an immunotherapeutic challenge. According to Fan and co-workers (Fan et al.), regulatory T cells (Treg) may play key roles in the creation of an immunosuppressive environment that favors activity of PDAC in the TME. Critical immune evasion mechanisms employed by PDAC cells involve downregulation of Major Histocompatibility Complex (MHC) class I molecules and the expression of genetic mutations in MHC Class I/II molecules that would result in erratic antigen presentation (Ryschich et al.; Pandha et al.; Birnbaum et al.). Furthermore, immune tolerance is observed in most PDAC patients, largely due to atypical expression of Fas receptor and Fas ligand. Ideally, normal healthy pancreatic epithelial cells possess only the Fas receptors but not the ligand. However, PDAC cells possess both - the Fas receptor in PDAC cells, albeit non-functional, exhibits some form of resistance to Fas-mediated apoptosis, while the ligand largely induces programmed cell death in immune effector cells (von Bernstorff et al.). Also, PDAC cells are responsible for recruiting immunosuppressive TAMs and myeloid-derived suppressor cells (MDSCs) via the C-C motif chemokine ligand 2/ C-C motif chemokine receptor 2 (CCL2/CCR2) axis from peripheral circulation (Sanford et al.). They also express increased levels of CCL5 to facilitate recruitment of Treg cells, suggesting that Treg cells are recruited to lesions associated with PDAC (Tan et al.; X. Wang et al.). PDAC cells can facilitate the degradation of tryptophan, which is essential for the survival and activation of T cells, by producing the enzyme indoleamine 2,3-dioxygenase (IDO), leading to apoptosis and anergy of T cells (Uyttenhove et

al.; Peng et al.). These accentuate the role of PDAC epithelial cells in immunosuppression, but another critical component of PDAC in the TME that facilitates suppression of immunotherapeutic strategies is the stroma. In fact, according to Neesse and co-workers (A. Neesse et al.; C. Feig et al.), the stroma makes up about 90% of the PDAC tumor mass. The stroma facilitates the progression of fibrosis and inhibits delivery of antitumor regimens (Hwang et al.; Lonardo et al.), even to the extent of inactivating cytotoxic T cells and increasing the number of immunosuppressive cells (Wörmann et al.; Zheng et al.). At advanced stages of the diseases, the number of PSCs also increase. PSCs are a special type of cancer-associated fibroblast (CAFs) associated with PDAC (Shi et al.). Upon activation, these cells produce CXCL12 which inhibits the infiltration of $CD8^+$ T cells in the stroma, but not in the cancer nests (Ene-Obong et al.). These PSC cells can also induce T-cell anergy and apoptosis by expressing galectin-1 (Tang et al.). The stroma, therefore, serves as a significant barrier against anti-tumor immune functions, and thus targeting the TME can be an innovative means to improve access of effector immune cells to PanCa, particularly in PDAC. Unfortunately, attempts at immunotherapy in PanCa, to date, have not achieved any significant clinical benefits as stand-alone treatment.

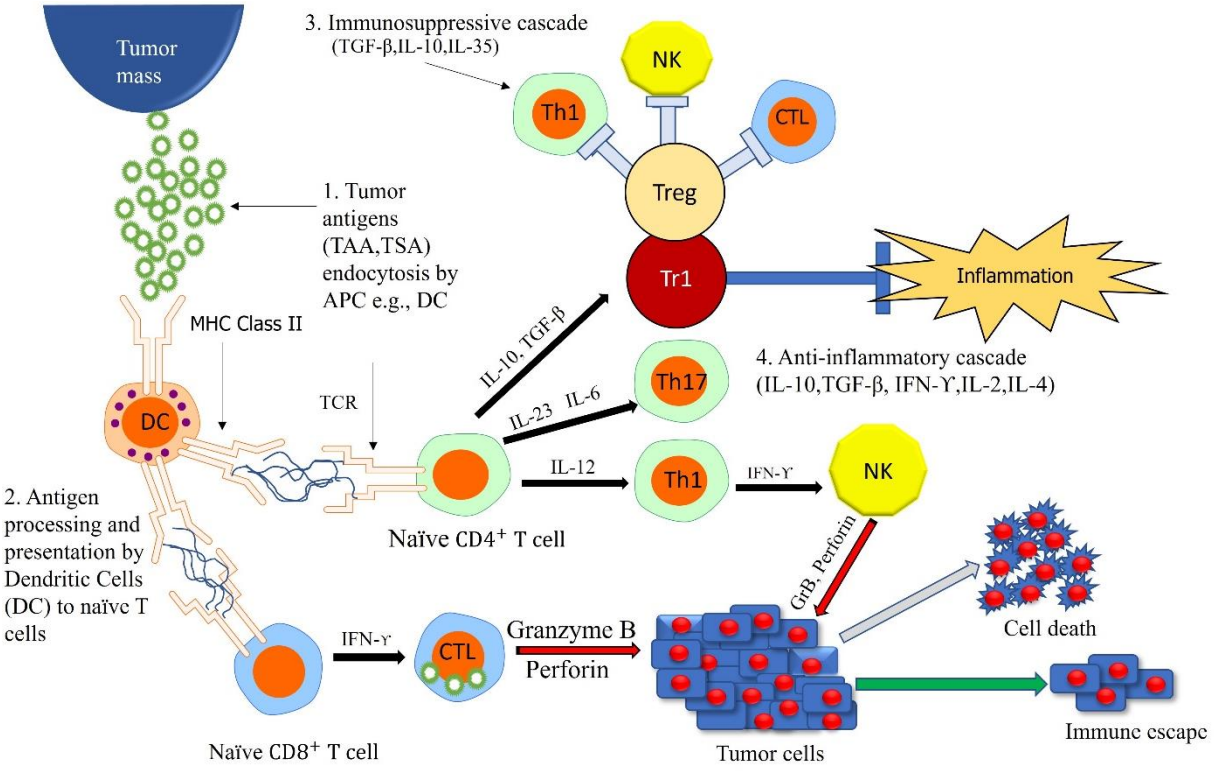

Figure 2-2**.** PDAC carcinogenesis and subsequent advancement triggers the swing from predominantly inflammatory immune cells to immunosuppressive populations. At early PDAC stages, T-cell receptor (TCR) activation by Antigen Presenting Cells (APCs) activates downstream signaling pathways and consequently leads to immature T cell proliferation and maturation into immune effector cells. A basic anticancer immune cell network ensures effector T and Natural Killer (NK) cells delimit proliferation of tumors. Critically, some primed T lymphocytes remain inactive and can be activated and differentiated into Tregs, just as non-primed lymphocytes. Tregs release immunosuppressive cytokines that inhibit activity of Cytotoxic T lymphocytes (CTLs), T helper 1 (Th1) and NK cells. T regulatory 1 (Tr1) cell release anti-inflammatory cytokines which dampen the pro-inflammatory response initiated by T helper 17 (Th17) cells.

Current Treatment Modalities for PDAC

The five-year survival rate for PDAC has been sub-par (<10%), even though breakthrough in detection strategies and therapeutic modalities have gradually ameliorated clinical outcomes associated with this fatal malignancy (Siegel, Naishadham and Jemal). Survival rates are characteristically classified, as demonstrated in SEER records, into either localized, regional, or advanced disease. As such, the five-year survival range for localized disease (37.4%) drops down drastically to just 2.9% with advanced/metastatic cancers (Engbang et al.). Surgical resection as an arm of treatment sequencing appears to be the ideal curative measure, but more than 80% of patients with advanced diseased are classified as inoperable upon diagnosis (Sclafani et al.). Even for surgically resectable candidates, local disease recurrence is very prevalent (Zhang, Sanagapalli and Stoita). Recent studies have shown, however, that immunotherapy strategies have yielded enormous successes in treating PDAC (Schizas et al.), with some researchers even employing nanoscale drug delivery systems to enhance targeted disease therapy of PDAC (Sengupta et al.).

Immunotherapy of PDAC

This strategy deploys monoclonal antibodies to actively target immune checkpoint molecules through inhibition of Cytotoxic T-Lymphocyte–associated Antigen 4 (CTLA-4), Programmed-cell Death protein-1 (PD-1) and Programmed-cell Death protein Ligand-1 (PD-L1) (Brower). This has impressively led to a paradigm shift in the treatment of melanoma, lung cancer, renal cell carcinoma, among other malignancies (Brower). This approach offers an alternative therapeutic response beyond surgery, radiation therapy and chemotherapy.

However, there has been relatively little success in the use of immunotherapy in treating PanCa, as opposed to other types of malignancies, with the incredibly dense tumor microenvironment of PanCa serving as a major obstacle to the effective deployment of immunotherapy in targeting PanCa cells (Torphy, Zhu and Schulick). This has revolutionized the need to adopt combative and much more effective immunotherapeutic strategies to navigate this drawback (Torphy, Zhu and Schulick). Commonly used immunotherapeutic treatment modalities in PDAC therapy include immune checkpoint inhibition using inhibitors such as Ipilimumab, Pembrolizumab, Tremelimumab and Atezolizumab; therapeutic vaccines, and adoptive cell transfer such as Adoptive CAR-T cell therapy (Fan et al.). Other studies employ combination treatments of either treatment option such as adoptive cell transfer with whole cell vaccines, vaccines with immune checkpoint blockade etc. Various clinical studies involving combination therapies in PDAC immunotherapy have shown promising results. A combination therapy of ipilimumab and GEM was examined in a phase Ib clinical trial (NCT01473940), and preliminary data obtained demonstrated a median progression-free survival (PFS) of 2.5 months (95% CI 0.8–4.8) and median OS of 8.5 months (95% CI 2.2–10.3) (Schizas et al.). Among 11 patients, two exhibited partial response (PR) and five had stable disease (SD). Issues of toxicity were largely hematological. Further, clinical trials involving a combination therapy of ipilimumab with nivolumab (an anti PD-1 agent) is still ongoing with encouraging results (Schizas et al.). Moreover, in a phase I trial (NCT00556023), Aglietta et al. (2014) examined the potency of Tremelimumab when administered with GEM and the tumor response was assessed in 34 patients. 28 of the patients had a median OS of 7.4 months (95% CI 5.8–9.4).

Two patients showed PR and 7 patients had SD for >10 weeks with manageable levels of toxicity (Aglietta et al.). Furthermore, combination therapies of vaccines with immune checkpoint inhibitors have been quite successful in PDAC therapy. One phase I clinical trial assessed the efficacy of ipilimumab as a single agent as opposed to ipilimumab + GVAX in locally advanced and metastatic pancreatic tumors. This study recruited 30 randomly selected patients in a 1:1 ratio of either high-dose ipilimumab (10mg/kg) in one group, and ipilimumab + allogeneic PDAC malignant cells transfected with GM-CSF cell-based vaccines (GVAX) in the second group (D. T. Le et al.). The results accrued presented strong evidence regarding increasing efficacy of the combination therapy. The combination therapy was also found to be safe and tolerable and exhibited disease control in a total of 5 patients. Two single agent ipilimumab-treated patients in one arm posted SD at 7 and 22 weeks, while three patients administered with the combination therapy of ipilimumab + GVAX had prolonged SD at 31, 71 and 81 weeks respectively (Dung T Le et al.). Other combination therapies have explored Tremelimumab (Aglietta et al.), Pembrolizumab and Atezolizumab (Schmid et al.) as single agents and combination therapies in PDAC therapy. The major limitation to immunotherapy, however, is the barrier posed by the strong desmoplastic stroma and immunosuppressive TME that can possibly impede entry of T cells potentially targeted at eliminating the tumor cells.

Challenges of PDAC Therapy

Effective, minimally toxic systemic therapy for PDAC remains a continually unmet need. Over the years, surgical resection, chemotherapy, and radiation therapy have been employed in the treatment of PanCa with limited degrees of success (Stathis and Moore).

The major barrier to success to these treatment modalities has been attributed to the immunosuppressive TME that poses a major obstacle to effective antigen-presentation, and

subsequent infiltration by T effector cells (Ino et al.). Moreover, PDAC cells employ impressively shrewd immune evasion mechanisms that enable them to avoid immune scrutiny, while simultaneously facilitating and promoting growth, invasion, angiogenesis, and metastasis in host (Wörmann et al.). This pertinent eccentricity of PDAC cells and their associated microenvironment has been the major bane to deployment of conventional systematic therapy of PanCa, even though such conventional therapies have chalked immense success in treating other types of carcinomas such as melanoma and lung cancer. Various strategies have been touted to overcome these challenges in PDAC therapy. One strategy is Next Generation Sequencing (NGS). NGS presents a sustainable strategy of identifying vital somatic and germline genetic aberrations that underpin PDAC development and progression (Anteneh A Tesfaye et al.). NGS may facilitate identification of specific patient groups that require specialized therapeutic modules and help discover novel therapeutic targets that may help redesign treatments tailored to specific mutations (Anteneh A Tesfaye et al.). This is particularly crucial because according to Tesfaye et. al., (2018), there are presently no therapeutic agents that specifically target the four prominent mutations, proto-oncogene K-RAS, and the tumor suppressors, SMAD4/DPC4, TP53 and P16/CDKN2A in PDAC (Anteneh A Tesfaye et al.). These mutations have an incredibly low rate of prevalence in PDAC (Kleeff et al.) and as such, are not factored in clinical studies unless enrolled in mutation-specific clinical trials (Biankin, Piantadosi and Hollingsworth). Also, another challenge is the design of clinical trials based on patients with PanCa.

This is because PanCa is rare, and as such it is incredibly hard to accrue a large sample size of patients, particularly those with PDAC (A. A. Tesfaye et al.)

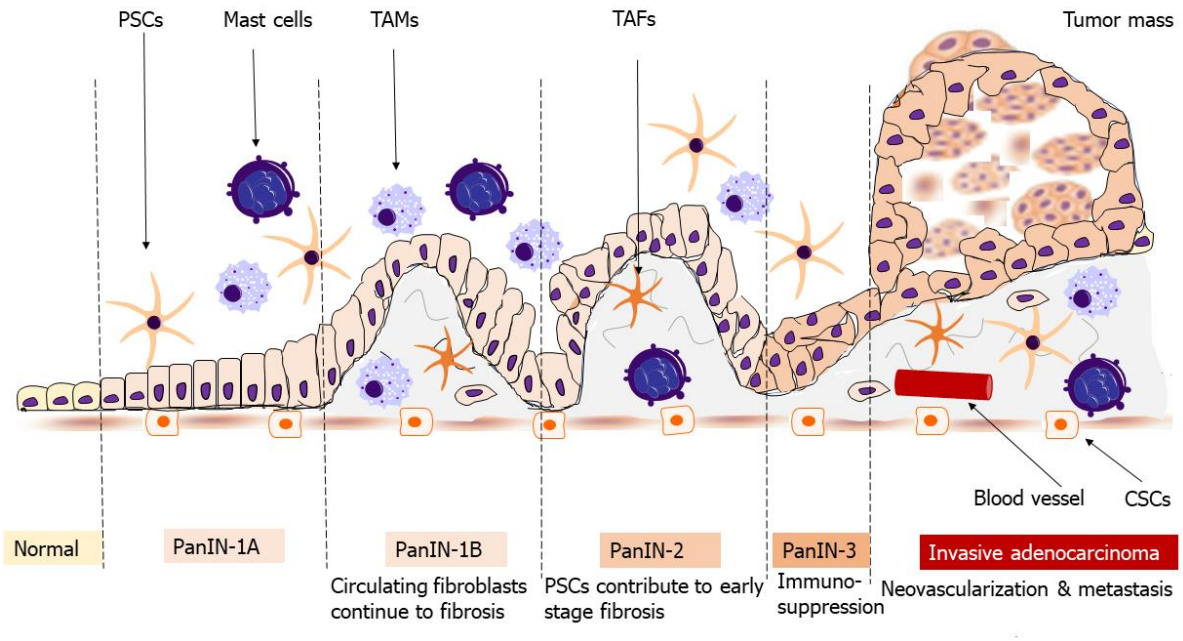

Figure 2-3. Schematic diagram of PDAC progression from normal cells to invasive adenocarcinoma in mammalian tissues.

Nano Immunomedicine

Conventional chemotherapeutics face challenges regarding the delivery of effective concentrations directly to pancreatic tumors without extensive systemic toxicities. In recent years, the generation of nanomedicines has afforded researchers the luxury of developing creative strategies for sustained drug delivery at tumor sites (Sahoo and Labhasetwar; Park et al.; Fortina et al.; Grodzinski, Silver and Molnar; Vasir and Labhasetwar "Targeted Drug Delivery in Cancer Therapy"; Vasir and Labhasetwar "Polymeric Nanoparticles for Gene Delivery"; Sengupta et al.). Drug delivery systems at the nanoscale level such as liposomes, polymers, and

other NPs, have yielded promising novel insights for enhanced encapsulation and sustained delivery of anti-tumor agents (Sahoo and Labhasetwar; Park et al.; Jain et al.; Vasir and Labhasetwar "Targeted Drug Delivery in Cancer Therapy"; Vasir and Labhasetwar "Polymeric Nanoparticles for Gene Delivery"). Nanoparticles are about 100-300nm in size and are ideal for drug delivery. This is because they selectively accumulate at tumor sites due to the leaky vasculature of the TME network, in a phenomenon termed as the Enhanced Permeation and Retention (EPR) effect (Bertrand et al.; Acharya and Sahoo). As such, nanotherapeutic formulations present distinct advantages over conventional approaches such as chemotherapy and radiotherapy in clinical cancer studies. Prominent nano formulations of conventional anti-cancer agents include Abraxane®, Doxil, Genexol-PM, CALAA-01, MCC-465, MBP-426, and BIND-014, and these have gained clinical approval by FDA for applications in clinical trials (Kamaly et al.). The goal of nanoencapsulation of therapeutic drugs is basically to enhance pharmacokinetics and efficacy of the drugs while concurrently decreasing systemic toxicity. Further, nanoencapsulation may improve the poor water solubility of certain therapeutic compounds and can serve as a multi-drug delivery carrier system (L. Zhang et al.). As a result of their relatively miniscule sizes, nanomedicines can selectively target solid tumors by exploiting irregularities in the TME vasculature (T. Stylianopoulos et al.; Sapra and Allen). The surface properties of NPs such as surface charge, shape and size regulate the passive accumulation of NPs in tumor tissues via the EPR effect (Acharya and Sahoo). This facilitates interrogation between the NPs and tumor cells after surface modification with targeting ligands. This improves selectivity and limits off-target toxicity associated with conventional chemotherapy. Thus, nano formulations of therapeutic drugs used to treat PDAC presents an intriguing therapeutic modality

with the potential to augment the therapeutic efficiency of drugs and can potentially mimic cell-cell interactions to enhance tumor cell uptake (Chen, Wang and Gu). As such, nanomedicine formulations can distinctly evade biological barriers, protect their inherent payload from enzymatic or other forms of degradation, and achieve targeted delivery to tumor sites (El-Zahaby, Elnaggar and Abdallah).

Nab-Paclitaxel

PTX mixed with albumin extracted from human serum in an aqueous solvent, forms a 100–200 nm drug nanoparticle in the form of albumin bound paclitaxel (nab-paclitaxel) (Frese et al.). Nab-paclitaxel has been studied thoroughly for its therapeutic potential in other types of cancers such as breast cancer (Schmid et al.), ovarian cancer (Parisi et al.), prostate cancer (Shepard et al.) and non-small-cell lung cancer (Kenmotsu et al.), and has been trialed for PanCa in multiple studies (Von Hoff et al.; Palacio et al.; Hosein et al.). Clinical studies (phase I/II and phase II) on the therapeutic potential of nab-paclitaxel yielded disparate results (Hosein et al.; Von Hoff et al.). The nano formulation exhibited promising competency in the first study but yielded discouraging results from the second study - promising beneficial effects of a combination of nab-paclitaxel and GEM were reported in the first study (Von Hoff et al.). The second study involved patients with advanced PanCa, and this study failed to show convincing therapeutic effect of this medication (Hosein et al.). As such, novel nano formulations such as PPNPs would present an added advantage over current nano formulations such as Nab-paclitaxel by chemo sensitizing the TME to GEM therapy via a mechanism mediated by Pluronic F127 to improve therapeutic outcomes.

Future Directions on PDAC Therapy

Although PanCa, and as such PDAC, remains a highly recalcitrant disease, the introduction and sustained utilization of nano formulations presents a new field of clinical potential and relevance to the generation of effective pathways and modalities aimed at treating this disease. Future research must focus on the development and advancement of efficient early detection strategies for PanCa to decrease mortality due to late detection of disease. Further, deployment of more up-to-date targeting of therapeutic agents is needed along with relatively simple ways to clinically test them for approval and marketing. It is quite unfortunate that most synthetic drugs that have demonstrated immense potential to combat PanCa have not yet been designed and implemented into nanocarrier systems. It is hoped that advancements in research, including research on anti-cancer agents and nanotechnology, might offer promising modalities to resolve issues of chemoresistance and offer new hope for PanCa immunotherapy. In addition, an exploration of nature's resources can help discover new anti-neoplastic agents, and by incorporating them into nano-carrier delivery systems, would offer a new weapon in the quest to solve the problem of resistance and decrease or eventually eradicate systemic toxicity. The field of exploiting nanocarriers in cancer treatment is promising for future research in PanCa therapy, but it is important to understand the field of nano-toxicology. Recent publications on nanomedicines have failed to cover long term toxicity studies (including organ accumulation especially in the kidney). According to El-Zahaby et al (2019), development of novel multifunctional nanoparticles that can combine the capabilities of diagnosis and treatment of PanCa, in addition to, monitoring the drug delivery and distribution would be ground-breaking. It is the hope that future research into nano-immunotherapy will yield considerable progress in the fight against PanCa, particularly PDAC.

CHAPTER III

DEVELOPMENT AND PHYSICOCHEMICAL CHARACTERIZATION OF PACLITAXEL LOADED PLGA NANOPARTICLES (PPNPs)

Materials and Methods

Synthesis of PPNPs

Synthesis of PPNPs was carried out using a modified protocol as previously described (Figure 3-1). Here, an aqueous solution of 1% Poly vinyl Alcohol (PVA) (Sigma, P8136) was prepared separately. Then, a solution of PLGA (Lacteal Polymers, B6010–4) in acetone (90 mg/5 ml) was also prepared in two separate vials, one for PLGA control and the other for PPNPs. Upon dissolution of PLGA in acetone, 10 mg of PTX (Advanced ChemBlocks, F-4194) was added to one of the vials with the PLGA-acetone mixture to yield PPNPs. As such, there were two different mixtures now: one with just PLGA mixed in acetone and the other with PLGA-PTX mixed in acetone to generate PPNPs. Next, each mixture (PLGA vehicle control and PPNPs) was added dropwise to individual PVA solutions then stirred overnight at 800-900 rpm while the container was loosely covered with foil to facilitate acetone evaporation. After 24 h, 5 mg/ml of Poly L-Lysine (PLL) (Sigma, P2636) and Pluronic F127 (Sigma, P2443) was prepared using Milli-Q water and 2 ml of the resulting solution added dropwise to each vial (PLGA vehicle control and PPNPs).

Each formulation was then stirred for 7 h, then diluted to 20 ml with Milli-Q water. Each vial was then aliquoted into 1.5 ml tubes and stored at −20°C. One tube each of PLGA vehicle control and PPNPs was transiently sonicated using a probe sonicator (MISONIX Inc.) to ensure thorough homogeneity for characterization.

Characterization of PPNPs

Particle Size. A JEOL-1210 transmission electron microscope (TEM) (JEOL Ltd., Tokyo, Japan) that was set at 60 kV was employed to ascertain the particle size and surface morphology of PPNPs. Here, 50 µL suspension of 1 mg/mL PPNPs preparation was gently pipetted unto a 200 mesh formvar-coated copper TEM-grid (grid size: 97 µm) (Ted Pella, Inc., Redding, CA), and then subsequently stained with 2% w/v uranyl acetate stain. The grid was then air-dried after 1 h to clear excess stain, then TEM imaging of stained particles on the TEM-grid. Also, Dynamic Light Scattering (DLS) analysis was used to further ascertain particle size and charge.

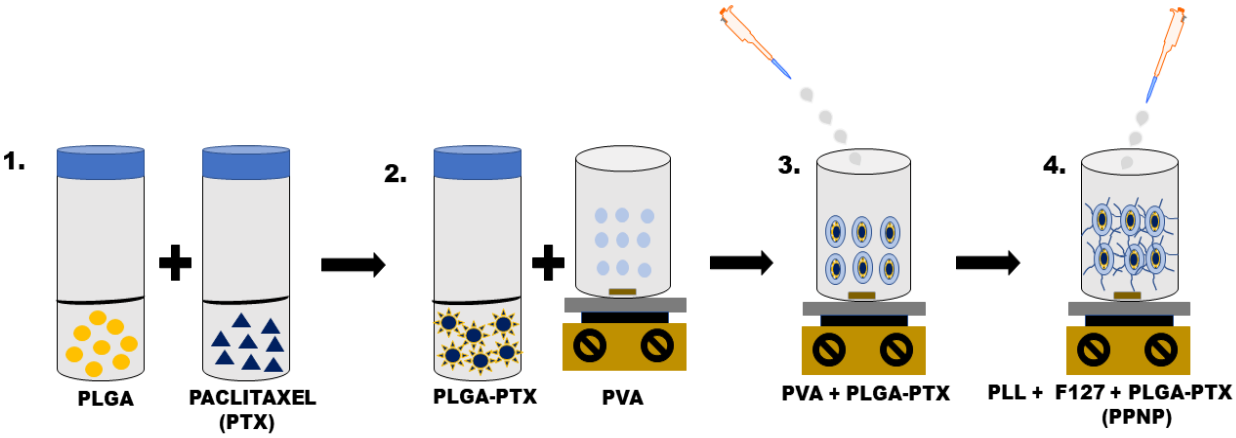

Figure 3-1. Diagram showing preparation method (nanoprecipitation) of PPNPs

Drug Loading. For drug loading analysis of PPNPs, freshly prepared PPNPs samples were spun thrice at 20,000 rpm for 120 min at 4º C using Eppendorf Centrifuge 5920R, then re-suspended in high-grade purified water and sonication on ice for 1 min. The supernatant was then discarded, leaving the pellet. Next, the pellet was re-suspended, lyophilized, and PPNPs from the pellet was extracted using 1 ml of acetonitrile for 48 h. Then, an UltiMate high-performance liquid chromatography (HPLC) (Dionex Corporation) equipped with UltiMate 3000 injector, RS variable wavelength detector, and an Acclaim polar advantage column of 3 µm 120 Å (4.6 × 150 mm) was employed to determine and analyze the concentration of PPNPs in the extract. The mobile phase of the extract contained a mixture of 1% citric acid: acetonitrile (40:60, v/v). An auto injector (Model 508, Beckmann Instruments) was used to inject 50 µL of the extracted samples for analysis of peaks using a UV detector with a wavelength of 279nm. The retention time was examined at ~18-20 min**.** A linear calibration curve in the range of 1 to 10 µg/mL was obtained at the same working condition for PPNPs. From this data, the PPNPs loading content was calculated as follows:

Fourier-Transform Infrared. Fourier-Transform Infrared (FT-IR) spectra of PPNPs were detected with an FT-IR microscope (Smiths Detection, Danbury, CT). The spectra data, 4,000–750 cm-1, was imaged at a cm-1 speed for 32 scans by placing lyophilized PPNPs powder on the attenuated total reflection objective. The final data is reported as mean of 32 scans.

Thermal Analysis. Thermal analysis of PPNPs was done via differential scanning calorimetry (DSC) and thermo-gravimetric analyzer (TGA) to ascertain physical status and thermal configuration of PPNPs. Both DSC and TGA profiles were carried out on a Q50 TGA (TA Instruments, New Castle, DE) under dry nitrogen atmosphere (a flow rate of 10 mL/min) from 25° C to 700° C at the heating rate of 10° C/min.

***In Vitro* Drug Release (Dialysis Bag Method).** Dialysis membrane bag-based drug release method was employed to evaluate release of PTX from PPNPs in PBS containing 0.1% (wt/vol) Tween-80 (PBS-T). In detail, 1 mL of 180 μg PTX/mL PPNPs suspension was placed in a dialysis membrane bag (molecular weight cut off size, 12 kDa, Sigma–Aldrich Co., St. Louis, MO) which was immersed in 3 ml PBS-T, pH 7.4 in a tube at 37° C and rotated at 100 rpm on an orbital shaker. The released drug from PPNPs into PBS-T was estimated at indicated time points [1 h, 3 h, 6 h, day 1 (24 h), day 3 (72 h), day 5 (120 h), and day 7 (168 h) using acetonitrile for drug extraction. The released PTX was analyzed by Waters HPLC Alliance system equipped with an e2695 separations module and a Waters 2998 photo-diode array (PDA) detector (Milford, MA, USA). Samples were analyzed using a Waters HPLC system which has an auto injector, and the instrument was operated by use of Empower2® software (Milford, MA, USA).

Components were separated on a Waters C18 reversed- phase column (Milford, MA, USA) with 300 mm × 4.6 mm dimensions and 5 μm particle size. A linear calibration curve in the range of 0.1 to 10 μg/mL was obtained as identical to drug release process and calculated the released drug from PPNPs formulation. The data is represented as percent release.

Colloidal Stability of Nanoparticles in Whole Human Serum Albumin (WHSA). In vitro stability of nanoparticles with human serum is critical to ascertain hemocompatibility of these formulations in vivo. Incompatible nanoparticles in human serum clump together and generate higher absorbance values. The Spectrophotometer absorption method was employed to analyze human serum compatibility of PPNPs since the serum is murky and DLS analysis would be inappropriate under such conditions. For this experiment, PPNPs was finally prepared at 1 mg/mL concentration; from this stock solution we incubated 100 μL of this novel formulation with 100 μL of whole human serum albumin at 37º C for different time points from 0 h to 48 h. At each time point, absorbance was measured at 560 nm utilizing Cytation 3 imaging multi microplate reader (Bio Tek).

Statistical Methods

Statistical analysis was determined by using an unpaired, two tailed student's t-test. The results were considered significant if $P< 0.05$. All graphs were generated using GraphPad Prism 5 software and Statistical Package for the Social Sciences, version 11.5 (SPSS Inc., Chicago, IL).

Results

Schematic Representation of Preparation of PPNPs

PPNPs formulation (Figure 3-2, A) has a variety of distinct properties. The FDA-certified biodegradable PLGA core can store and gradually release PTX, and PVA stabilizes the formulation for > 6 months and prevents off-target adsorption of systemic serum proteins [Massey, 2019 #2]. Also, PLL facilitates cellular internalization, has minimal toxicity relatively and serves as a charge enhancer while the amine functional groups on PLL aid in antibody conjugation (Massey et al.). Pluronic F127 polymer has been demonstrated to overcome drug resistance (W. Zhang et al.; Yallapu, Jaggi and Chauhan).

DLS Characterization and Zeta Potential for PLGA and PPNPs

DLS characterization showed a median particle size of 140 nm for PLGA and 160 nm for PPNPs (Figure 3-2, B) and demonstrated a moderately negative zeta potential (Figure 3-2, C).

FT-IR and XRD Spectra for Free PTX, PLGA, and PPNPs

Next, FT-IR and XRD analyses were performed to confirm uptake of PTX in PPNPs. FT-IR spectrum data from PLGA analysis (Figure 3-2 E, black line), exhibited intense peaks at 1000 cm-1, 1281 cm-1, and 1010 cm-1 because of C=O stretching of ester, C-O stretching of ester, and glycosidic (C–O–C/C–C/C–O) stretch vibrations (Massey et al.). Distinctive FT-IR and XRD peaks were observed for PTX (Figure 3-2 D/E, red line), but after drug encapsulation these sharp peaks were no longer noticeable in PPNPs (Figure 3-2, D/E, green line), which was strikingly like the PLGA vehicle control (Figure 3-2 D/E, black line). XRD analysis followed the same trend – PTX crystalline peaks were unnoticeable after drug encapsulation in PPNPs (Figure 3-2 D/E).

Characterization of PPNPs by Atomic Force Microscopy

Atomic Force Microscopy (AFM) imaging exhibited smaller particle sizes in the air (approximately 90-120 nm), possibly because of swelling in a liquid environment as observed with DLS (Figure 3-2, F, i–ii). In both PLGA and PPNPs, there was no significant difference in the modulus. However, there is a dearth of knowledge on the possible effects of other polymers in this particle system.

Drug Release Profile of PPNPs

PPNPs had excellent drug release profile with distinctive wavelength at 227nm, and a retention time of 112.02 seconds (Figure 3-2, G).

**Adapted with permission from Massey, Andrew E., et al. "Next-generation paclitaxel-nanoparticle formulation for PanCa treatment." *Nanomedicine: Nanotechnology, Biology and Medicine* 20 (2019): 102027.

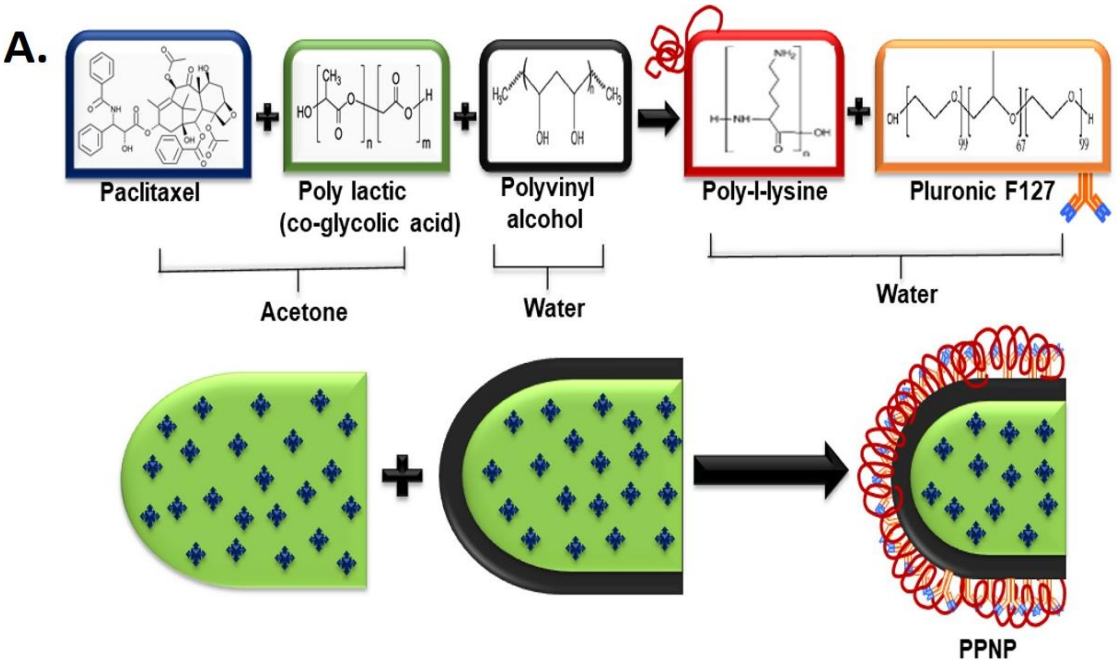

Figure 3-2 A. Schematic representation of preparation of PPNPs.

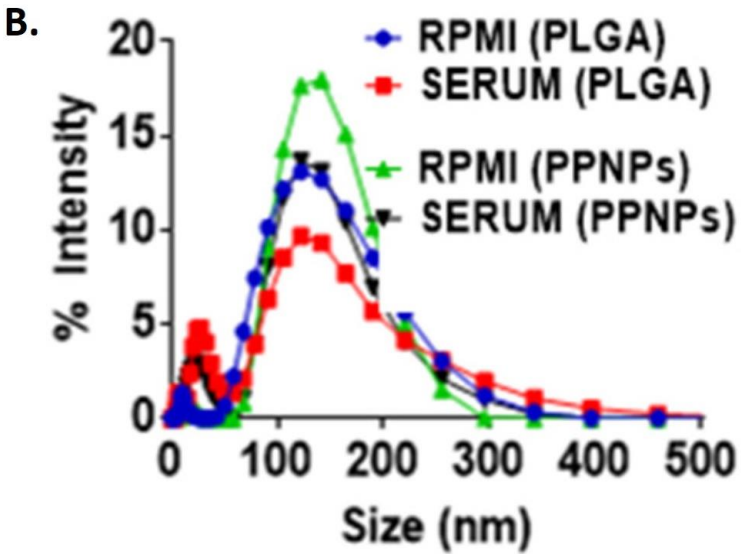

Figure 3-2 B. DLS characterization of PLGA and PPNPs.

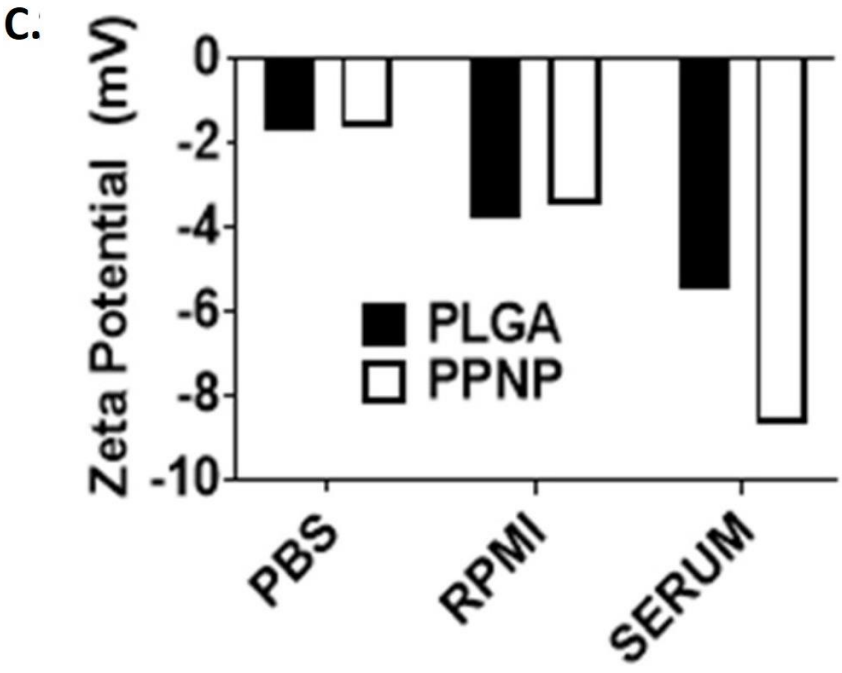

Figure 3-2 C. DLS characterization of zeta potential for PLGA and PPNPs.

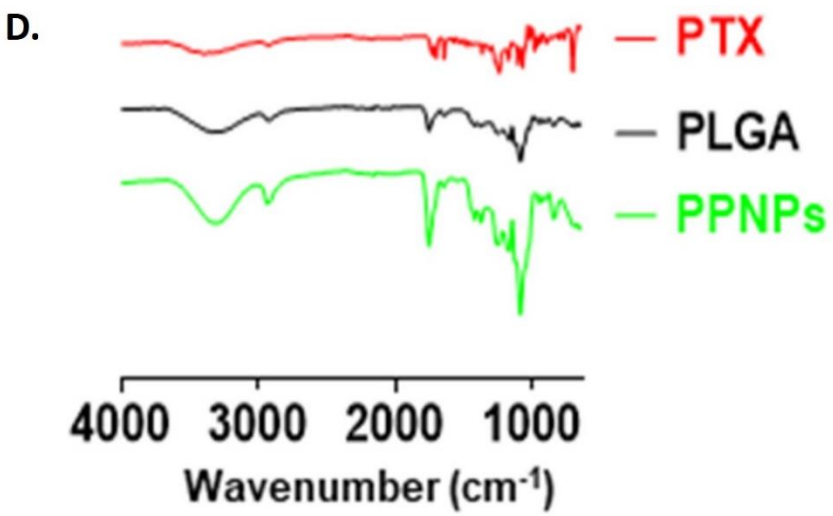

Figure 3-2 D. FT-IR spectra for free PTX, PLGA, and PPNPs

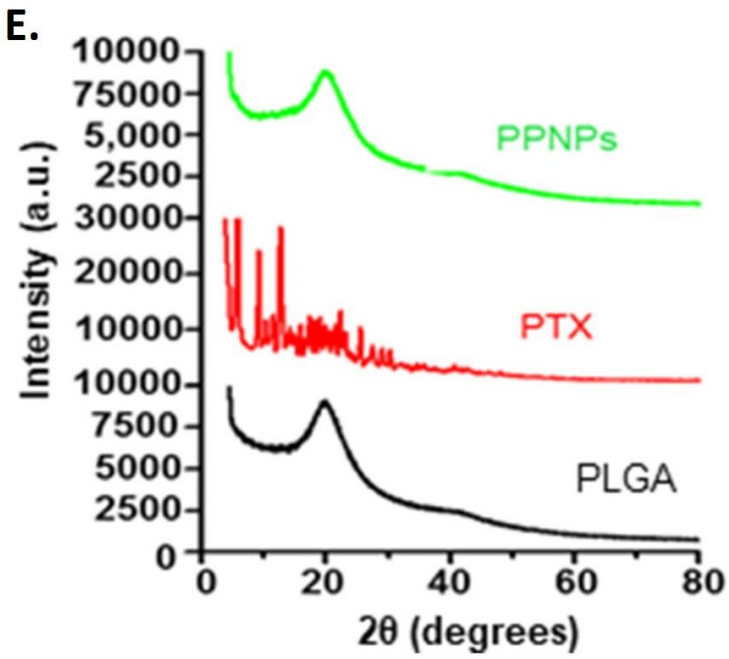

Figure 3-2 E. XRD spectra for free PTX, PLGA, and PPNPs

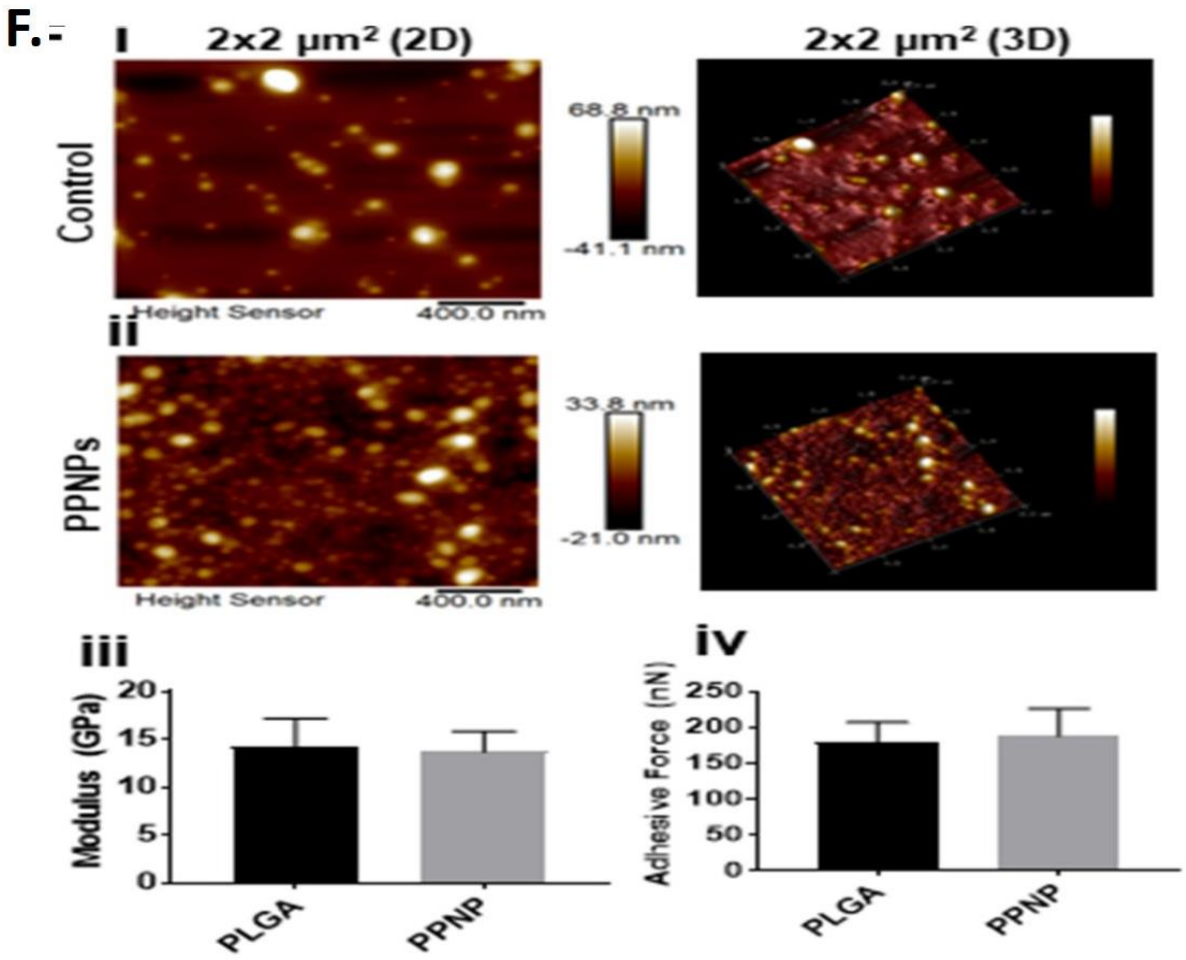

Figure 3-2 F. Topographical and physical analysis of PLGA and PPNPs by atomic force microscopy. Representative 2D and 3D images (2×2 μm^2) of PLGA and PPNPs (i-ii). Modulus data for two separate samples (iii-iv)

G.

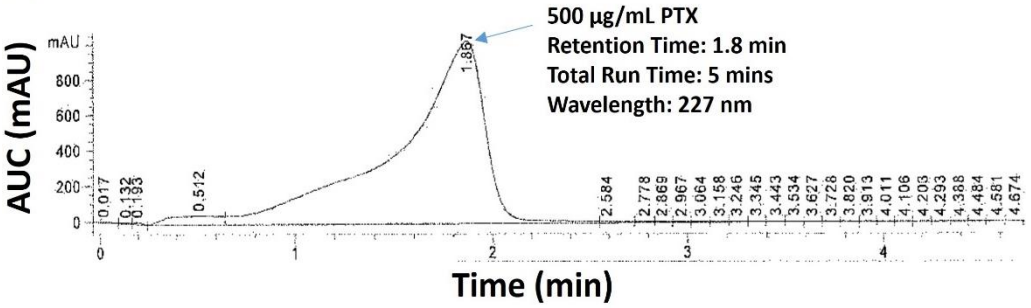

Figure 3-2 G. Drug release profile of PPNPs. Representative chromatograph of PTX with distinctive wavelength peaks and retention time (G).

CHAPTER IV

EVALUATION OF ANTI-PROLIFERATIVE ACTIVITY OF PPNPs IN PANCREATIC CANCER CELLS

Materials and Methods

Cell Culture

PanCa cell lines (Panc-1, HPAF-II, AsPC-1, MIA PaCa-2) were obtained from American Type Culture Collection (ATCC) (Manassas, VA, USA). These cell lines were cultured on appropriate media specified for each cell line, according to ATCC guidelines. Each media (RPMI, DMEM, DMEM-F12) was supplemented with 10% heat inactivated FBS (Atlantic Biologicals, Lawrenceville, GA, USA) and 5 mL 1X antibiotic/antimycotic. All PanCa cell lines were incubated at 37°C with 5% CO_2 humidity.

Cell Proliferation Assay

In the cell proliferation assay, PanCa cell lines (Panc-1, HPAF-II, AsPC-1, and MIA PaCa-2) were seeded at 5×10^3 cells/well density in 96-well plates and incubated at 37°C for 24 h to facilitate cell attachment. After incubation, the cells were treated with different concentrations of either free PTX or PPNPs nano formulations for 72 h. DMSO served as control and Poly (lactide-*co*-glycolide) (PLGA) without the drug were used as vehicle controls.

After 72 h, cells were imaged under an optical microscope to observe treatment effects. Images were captured with an Olympus microscope (Olympus, Center Valley, PA). Next, 20 µL of MTT (3-(4, 5-dimethylthiazolyl-2)-2, 5-diphenyltetrazolium bromide) reagent (Cell Titer 96 Aqueous, Promega Corporation, Madison, MI) were added to each well, and plates were incubated for 3 - 4h. After the incubation period and upon observation of crystal formation in all wells, the media was aspirated from all the wells and 100µL of DMSO added to each well. The well plate was then agitated gently for 15 min on a shaker to completely solubilize the crystals and the optical density (absorbance) for each well was recorded at 590 nm spectrophotometrically using a BioMate 3 microplate reader (Thermo Fisher Scientific, Pittsburgh, PA). Each experiment had 6 replicates for accuracy of results.

Colony Forming Assay

PanCa cell lines (Panc-1, HPAF-II, AsPC-1, MIA PaCa-2) were seeded at the density of 500 cells/well in 12-well plates and incubated at 37°C with 5% CO_2 for 24 h to facilitate cell attachment. Next, the cells were treated with different concentrations of either free PTX or PPNPs and subsequently incubated for 14–16 days. Poly (lactide-*co*-glycolide) (PLGA) without drug were used as vehicle controls. During plate termination, plates were washed twice with 1X PBS to remove dead colonies, fixed with ice-cold methanol (MeOH), stained with 0.5% crystal violet in 25% methanol, and washed with running distilled water. Plates were then air-dried and visualized with a gel doc (Bio-Rad, Hercules, CA). Colonies were counted using ImageJ (Image J software, NIH USA), and each experiment conducted in triplicates for accuracy of results.

Statistical Methods

Quantitative data were presented as mean ± standard error (SEM) in this study. Statistical analyses were conducted by using an unpaired, two-tailed student's t-test.

The results are considered significant if $P < 0.05$ ($\alpha = 0.05$). All graphs were generated using GraphPad Prism (5.03, GraphPad Software, Inc., La Jolla, CA, USA).

Results

PPNPs Treatment Inhibits Cellular Proliferation of Various PanCa Cells

A peculiar feature of cancer cells is their ability to over-proliferate into tumor masses that eventually results in establishment and development of tumors. The rate of proliferation of cancer cells is unmanageable at best. As such, a high-quality anticancer drug candidate should be able to impair cell proliferation. PPNPs demonstrated superior therapeutic efficacy in inhibiting cellular proliferation of PanCa cells compared to free PTX in a dose-dependent (2.5–80 nM) manner (Figure 4-1). IC50 of PPNPs in Panc-1 was approximately 5 nM (Figure 4-1, A), while the IC50 was approximately 10 nM in HPAF-II (Figure 4-1, B), AsPC-1 (Figure 4-2, C) and MIA PaCa-2 (Figure 4-2, D) cells at 72 h.

PPNPs Treatment Inhibits Clonogenic Potential of Various PanCa Cells

Also, a major hallmark of cancer is the capability of a single cell to proliferate and establish large colonies. Gradual, continued release of PTX from PPNPs may exhibit long term inhibitory effects on cells and this was observed in the reduced colony forming ability of the cells after 14 days**.** It was observed that PPNPs sufficiently inhibited colony forming abilities of PanCa cells better than free PTX in a dose-dependent manner (Figure 4-3, A-D) with markedly significant differences observed at 2.5 and 5 nM concentrations ($p < 0.01$) of both drugs in Panc-1 (Figure 4-3, A, i), HPAF-II (Figure 4-3, B, ii), AsPC-1 (Figure 4-4, C, iii) and MIA PaCa-2, where there were no colonies remaining after the treatment duration (Figure 4-4, D, iv).

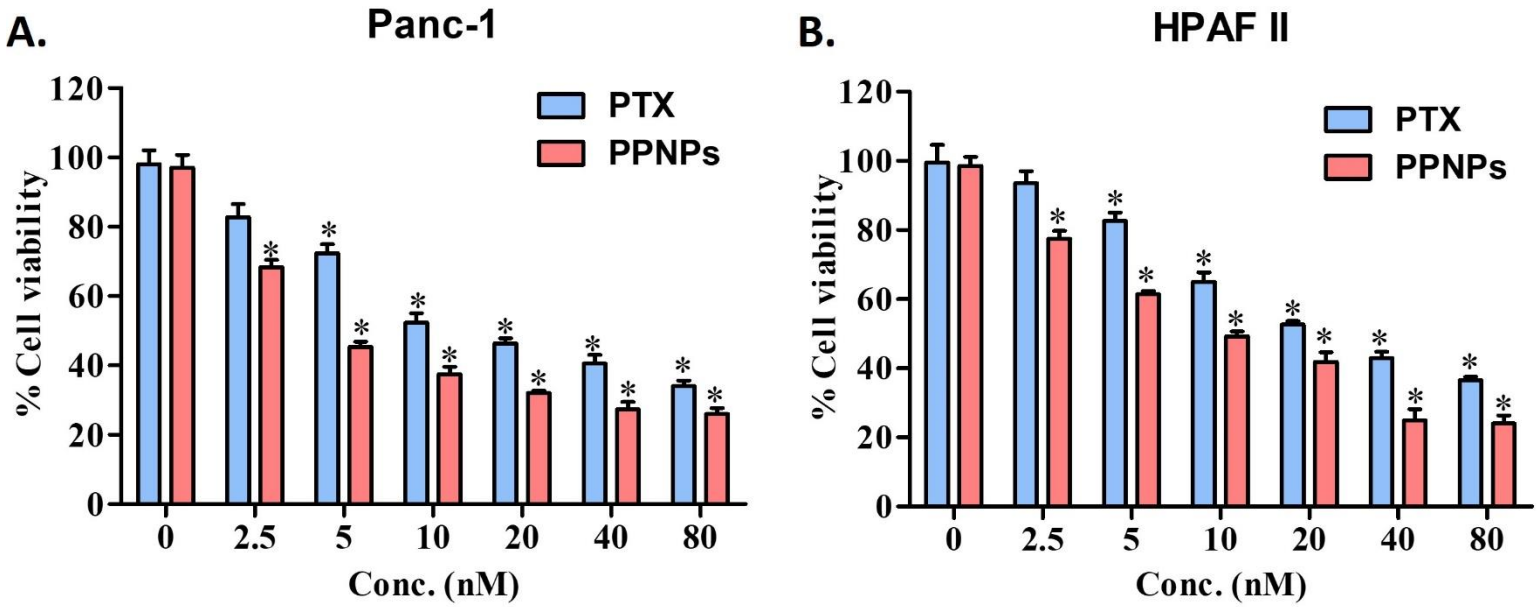

Figure 4-1. Effect of PPNPs on cell proliferation of PanCa cells. PPNPs inhibited cellular proliferation of Panc-1 (A) and HPAF-II (B). Values in bar graph represent mean ± SEM of 6 wells. Significant values = *$p < 0.05$.

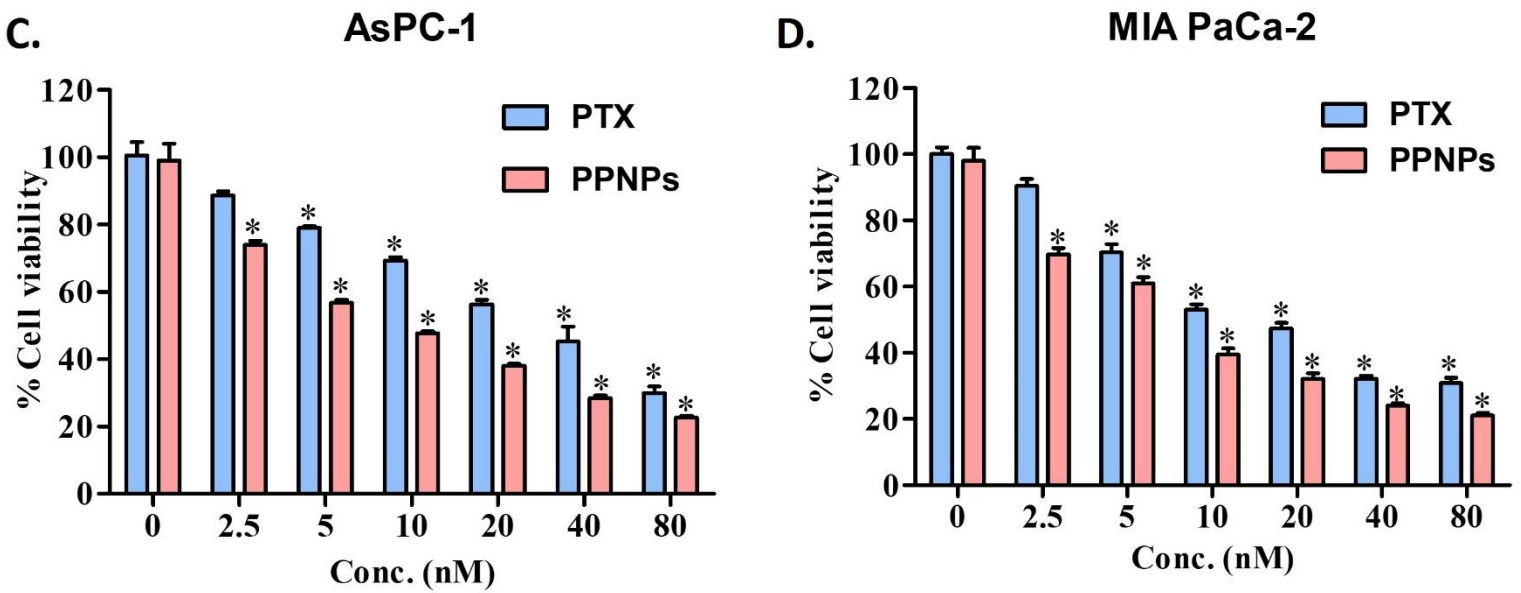

Figure 4-2. Effect of PPNPs on cell proliferation of PanCa cells. PPNPs inhibited cellular proliferation of AsPC-1 (C) and MIA PaCa-2 (D). Values in bar graph represent mean ± SEM of 6 wells. Significant values = *$p < 0.05$.

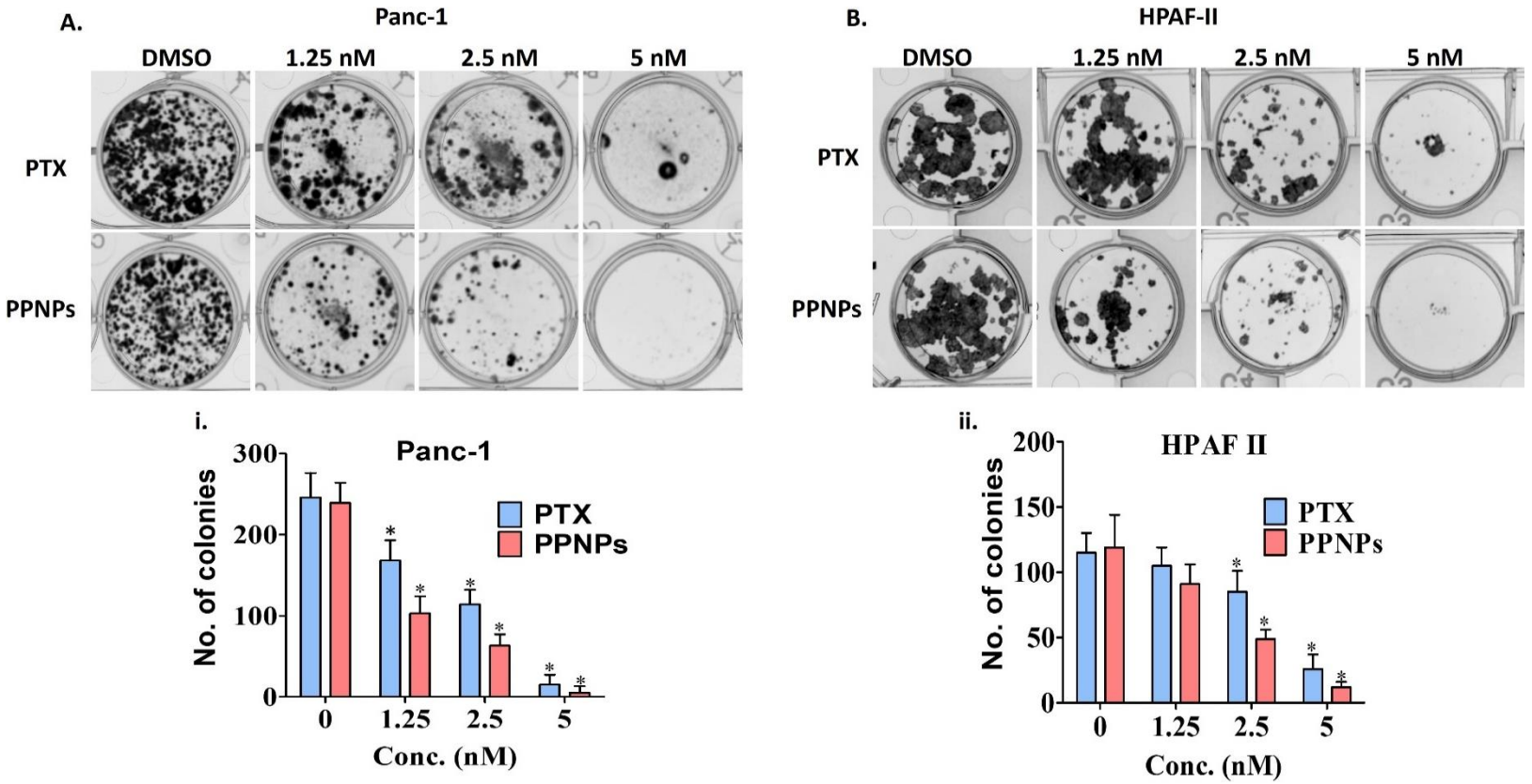

Figure 4-3. Effect of PPNPs on clonogenic potential of PanCa cells. Representative colony images of control and PPNPs treated groups of Panc-1 (A) and HPAF-II (B). Average colony counts in bar graph for Panc-1 (i) and HPAF-II (ii). Values in bar graph represent mean ± SEM of 3 wells. Significant values = *$p < 0.05$

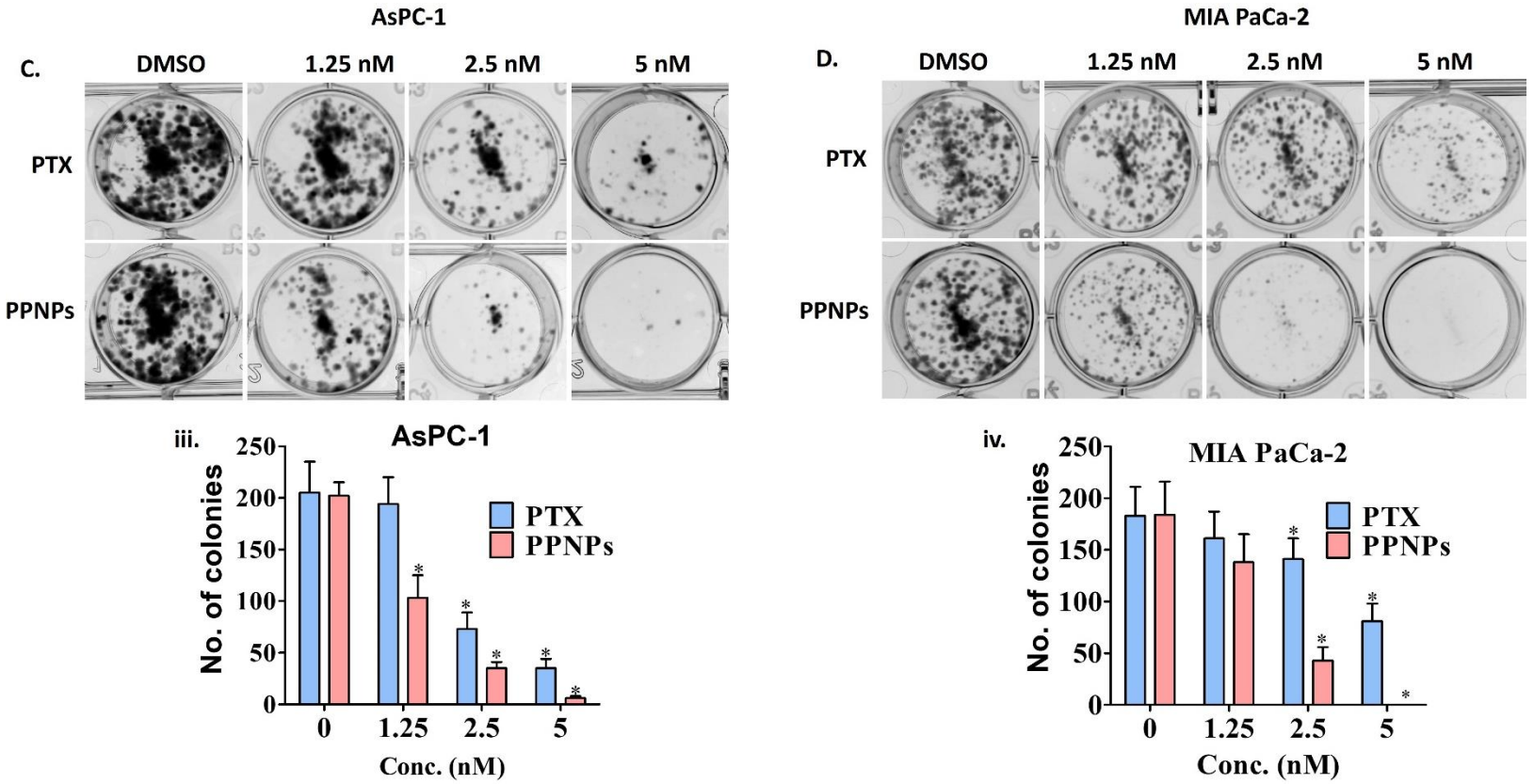

Figure 4-4. Effect of PPNPs on clonogenic potential of PanCa cells. Representative colony images of control and PPNPs treated groups of AsPC-1 (C) and MIA PaCa-2 (D). Average colony counts in bar graph for AsPC-1 (iii) and MIA PaCa-2 (iv). Values in bar graph represent mean ± SEM of 3 wells. Significant values = *$p < 0.05$

CHAPTER V

DETERMINATION OF EFFECT OF PPNPs ON APOPTOTIC PROTEINS IN PANCREATIC CANCER CELLS

Materials and Methods

Quantitative Real Time-Polymerase Chain Reaction

To assess the gene expression activity of PanCa cell lines treated with PPNPs, 1×10^6 cells were plated on 100 mm plates and incubated overnight for cellular attachment. Then, cells were treated with 10 nM concentration of PTX and PPNPs and incubated for 48 h. Next, the adherent cells were collected, and the total RNA extracted with the Qiagen RNeasy kit (Qiagen Inc., Valencia, CA, USA). Reverse transcription was performed with the High-Capacity RNA to cDNA kit and amplified with SYBR Green PCR master mix (both from Applied Biosystems). The cDNA was then amplified with specific primers based on the gene of interest. Each reaction was performed in triplicates with a MyiQ single-color real-time PCR thermocycler and analyzed with GeneX (Microsoft Excel macro provided by BioRad). An endogenous control, Glyceraldehyde 3-phosphate dehydrogenase (GAPDH) was employed as a normalization control. PLGA served as the vehicle control.

Immunoblotting

In this experiment, 2×10^6 cells were plated on 100 mm plates and incubated overnight for cellular attachment. Cells were then treated with 10 nM PTX or PPNPs for 48 h.

Then, cells were washed twice with 1X PBS, and 300µL of Sodium Dodecyl Sulfate (SDS) buffer (Santa Cruz Biotechnology, Santa Cruz, CA) containing 10 µL/ml each of protease/phosphatase inhibitors and Ethylenediaminetetraacetic acid (EDTA) added to each plate to lyse cells. Cell lysates were then collected by scraping cells with a cell scraper into 1.5ml centrifuge tubes. Lysates were subsequently sonicated for 30–40 s and spun at 15,000 rpm at 4 °C for 15min and supernatant collected. All steps were carried out on ice. Next, the Bradford Assay was employed to determine the quantities of protein concentration in each sample. 20 µg of protein from each treatment group was loaded and differentiated by 4–20% SDS-PAGE gel electrophoresis at 100 V for 80 min. Separated proteins were then transferred onto a poly (vinylidene difluoride) (PVDF) membrane and electrophoresed at 100 V for 80 min. The blots were then blocked with 5% non-fat milk in Tris buffered Saline with Tween 20 (TBS-T) at room temperature for 1 hour and subsequently incubated with specific primary antibodies at 4 °C for 24 h. Antibodies included components of various apoptotic pathways including B-cell Lymphoma-2 (BcL-2), BcL-2-associated X protein (BAX) as well as Cleaved Poly-ADP Ribose Polymerase (Cleaved PARP) and Cleaved Caspase-3. After incubation, the blots were washed three times with TBS-T for 5 min each and incubated with antirabbit/mouse secondary antibodies for an hour at room temperature. To detect protein signals, blots were washed again, three times with TBS-T for 15 min (5 min per wash), and then the blots were soaked in a Lumi Light reagent (Roche, Nutley, NJ) and visualized with a gel doc machine (BioRad, Hercules, CA).

Statistical Methods

Quantification of protein expression was done using GelQuant.Net from biochemlabsolutions.com. All graphs were generated using GraphPad Prism 5.

Results

PPNPs Modulate Expression of Key Apoptotic Proteins in Various PanCa cells

Apoptosis is a key regulatory event in the cellular developmental profile of any cellular organism. Apoptosis is programmed cell death that results in homeostatic balance of bodily cells in tissues via elimination of damaged cells and maintenance of a healthy population of cells required for growth and development (Elmore). In eukaryotes, apoptosis contributes to formation of digits and diminishing of the tail in higher mammals such as human beings (Elmore). In cancer cells, apoptotic pathways that regulate cellular proliferation are highly deregulated to ensure continued proliferation of these malignant cells and progression of disease. Anti-apoptotic are considerably over-expressed while pro-apoptotic proteins are downregulated concurrently. As such, we sought to determine the ability of PPNPs to sufficiently regulate key apoptotic proteins that dictate cellular developmental processes. It was observed that treatment with PPNPs significantly upregulated expression of pro-apoptotic proteins such as Bax, Cleaved PARP and Cleaved Caspase-3 while downregulating activity of anti-apoptotic proteins such as Bcl-2 compared to free PTX in both Panc-1 (Figure 5-1, A) and HPAF-II (Figure 5-1, B) cell lines**.** GAPDH served as the loading control.

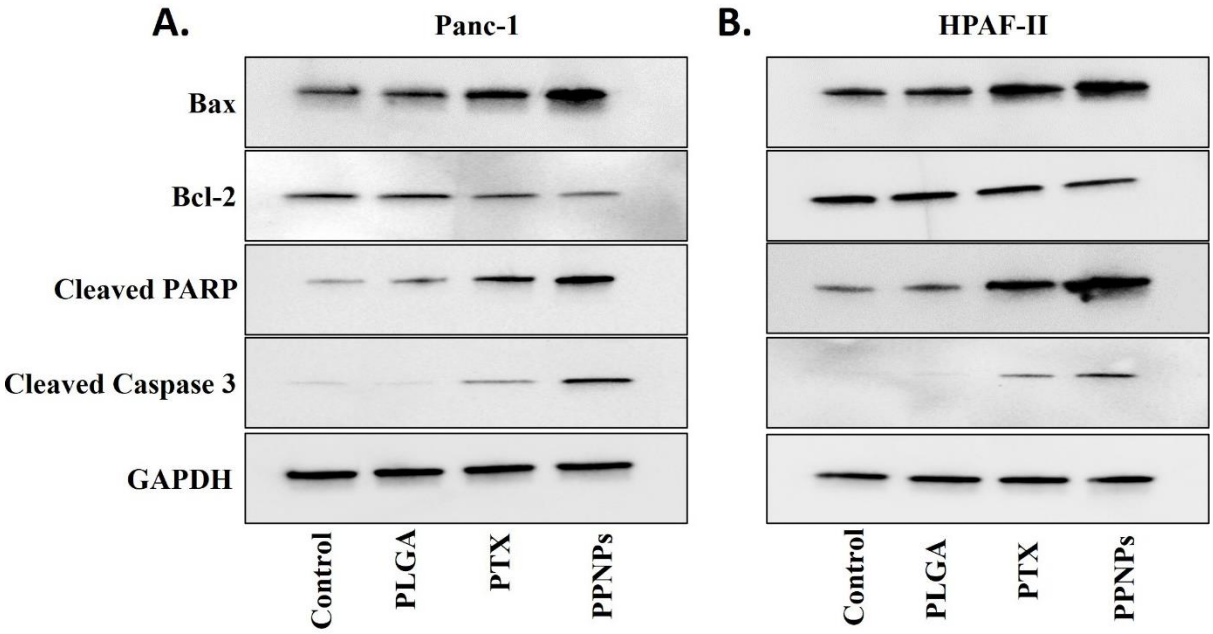

Figure 5-1. Effect of PPNPs on apoptotic proteins in PanCa cells. Western blot analysis of PPNPs-mediated regulation of expression of apoptotic proteins in Panc-1 (A) and HPAF- II (B) cell lines.

CHAPTER VI

DETERMINATION OF ANTI-MOTILITY PROPERTIES OF PPNPs IN PANCREATIC CANCER CELLS

Materials and Methods

Boyden Chamber Cell Migration Assay

Cell migration assay was performed in a 96 well format HTS transwell plate from Corning. All PanCa cell lines utilized (Panc-1, HPAF-II, AsPC-1, and MIA PaCA-2) were serum starved. Next day, 30,000 cells/well density of each cell line were seeded in the upper chambers containing serum free culture medium with 2.5 nM concentration each of PTX and PPNPs treatment prepared in serum-free media accordingly. Total volume of cell suspension, drug volume and serum-free media was 100 µL in each of the upper chambers. Seeded cells were then urged to migrate towards the lower chamber containing 250 µL media enriched with 10% FBS for 24 h. At the end of the indicated treatment period, cells were washed twice with 100 µL 1X PBS and subsequently fixed with 100 µL 4% paraformaldehyde prepared in 1X PBS for 20 min at room temperature and stained with crystal violet for 20 min. Plates were then washed with running distilled water to remove any excess stains. Cells that failed to migrate from the upper chamber were completely removed by cotton swab while wet, and this was carefully done to prevent swab from touching membrane of upper chamber.

Plates were then air-dried overnight, and migrated cells that were stuck on the membrane of the upper chamber were observed/ imaged by using light microscope (EVOS 7000) at 10X magnification. Each experiment was performed in triplicates for reproducibility of results.

Boyden Chamber Matrigel Cell Invasion Assay

For invasion assay, we used BD Bio coat Matrigel Invasion Chambers 24 transwell format (BD Biosciences). For this assay, PanCa cells to be seeded (Panc-1, HPAF-II, AsPC-1, and MIA PaCA-2) were serum-starved overnight. The next day, invasion chambers/inserts were filled with 500 µL serum free culture medium for 120 min at 37º C to activate the membrane of the inserts. 30,000 cells/well of each cell line was plated the next day in 500 uL serum-free media into the upper chamber/insert after activation. The lower wells were filled with 500 µL serum free media and the whole plate containing both upper and lower chambers was incubated at 37º C for 24 h for cellular attachment. Next day, PPNPs treatment at 2.5 nM concentration as well as PTX 2.5 nM prepared in 500 µL serum free media were administered to the seeded cells in the upper chambers, and the serum free media in lower wells was replaced with appropriate media enriched with 10% FBS. Cells were now urged to invade the Matrigel towards FBS gradient in the lower chamber for the next 24 h. After 24 h, the cells were washed twice with 500 µL 1X PBS and fixed with 500 µL of 4% paraformaldehyde for 20 min at room temperature. Next, fixed cells were stained with 0.5% crystal violet for another 20 min, washed with running distilled water, and air dried. Cells stuck on the membrane of the chamber/insert (invaded cells) were imaged at 10X magnification by using a light microscope (EVOS 7000).

Statistical Methods

Quantitative data were presented as mean ± standard error (SEM) in this study. Statistical analyses were conducted by using an unpaired, two-tailed student's t-test. The results are considered significant if $P < 0.05$ ($\alpha = 0.05$). All graphs were generated using GraphPad Prism (5.03, GraphPad Software, Inc., La Jolla, CA, USA).

Results

PPNPs Suppress Migratory Potential of Various PanCa Cells

Cellular migration and invasion are key features of cancer cells that facilitate metastasis to distal systemic regions away from site of local tumor to establish disease progression. Here, we sought to investigate the effect of PPNPs on the motility properties of PanCa cell lines. It was demonstrated that 2.5 nM concentration of PPNPs sufficiently inhibited cellular migration potential of Panc-1 (Figure 6-1, A), HPAF-II (Figure 6-1, B), AsPC-1 (Figure 6-1, C) and MIA PaCa-2 (Figure 6-1, D) in a significantly superior manner compared to free PTX at the same concentration.

PPNPs Suppress Invasive Potential of Various PanCa Cells

It was also demonstrated that 2.5 nM concentration of PPNPs sufficiently decreased the invasive potential of Panc-1 (Figure 6-2, A), HPAF-II (Figure 6-2, B), AsPC-1 (Figure 6-2, C) and MIA PaCa-2 (Figure 6-2, D) more efficiently than free PTX at the same concentration. DMSO served as a control and PLGA served as vehicle control for PPNPs for both experiments.

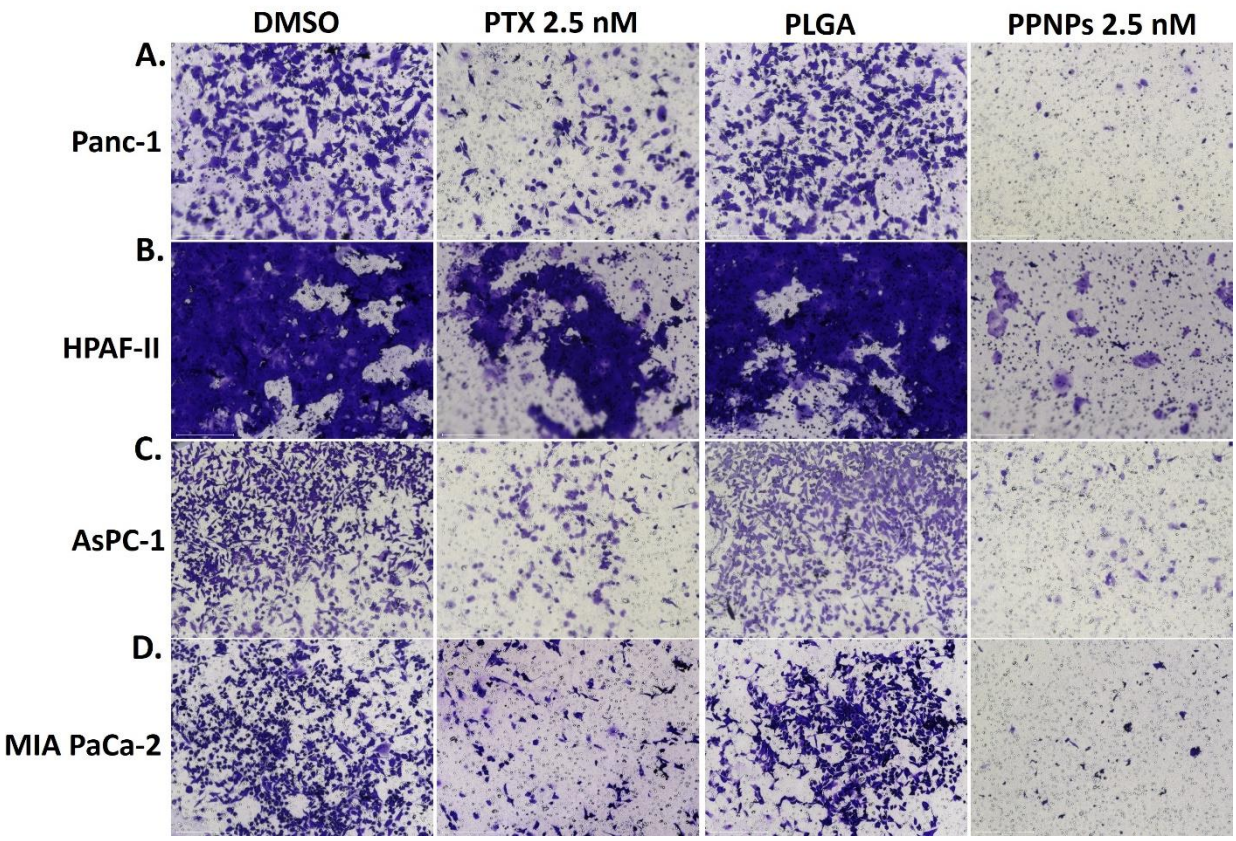

Figure 6-1. Effect of PPNPs on migratory potential of PanCa cells. Representative images showing the effect of PPNPs on migration potential of Panc-1 (A), HPAF-II (B), AsPC-1 (C) and MIA PaCa-2 (D) cell lines through Boyden-Chamber Migration assay.

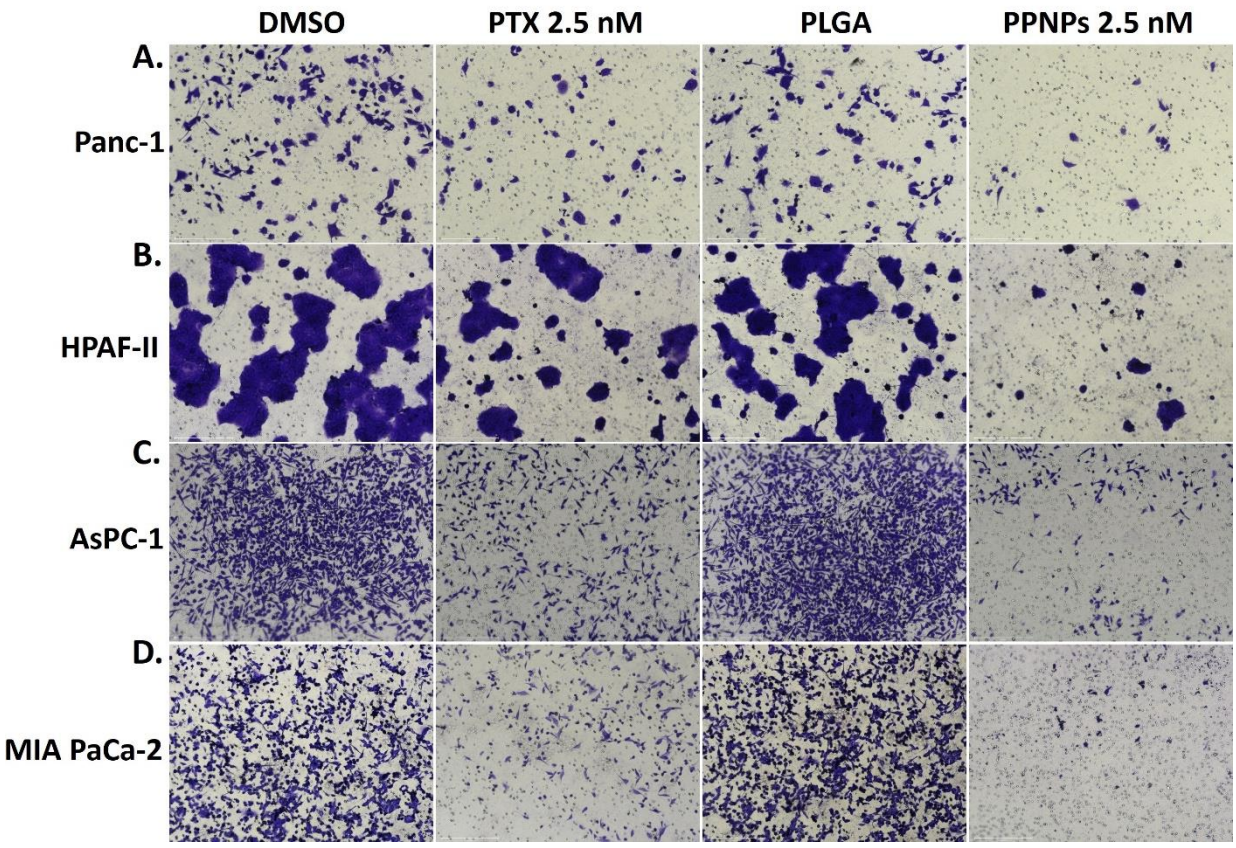

Figure 6-2. Effect of PPNPs on invasive potential of PanCa cells. Representative images showing the effect of PPNPs on invasive potential of Panc-1 (A), HPAF-II (B), AsPC-1 (C) and MIA PaCa-2 (D) cell lines through Boyden-Chamber Matrigel Cell Invasion assay.

CHAPTER VII

ANALYSIS OF EFFECT OF PPNPs ON EXPRESSION OF SONIC HEDGEHOG SIGNALING PATHWAY IN PANCREATIC CANCER

Materials and Methods

Quantitative Real Time-Polymerase Chain Reaction

To assess the gene expression activity of PanCa cell lines treated with PPNPs, 1×10^6 cells were plated on 100 mm plates and incubated overnight for cellular attachment. Then, cells were treated with 10 nM concentration of PTX and PPNPs and incubated for 48 h. Next, the adherent cells were collected, and the total RNA extracted with the Qiagen RNeasy kit (Qiagen Inc., Valencia, CA, USA). Reverse transcription was performed with the High-Capacity RNA to cDNA kit and amplified with SYBR Green PCR master mix (both from Applied Biosystems). The cDNA was then amplified with specific primers based on the gene of interest (SHH, PTCH-1, and Gli-1). Each reaction was performed in triplicates with a MyiQ single-color real-time PCR thermocycler and analyzed with GeneX (Microsoft Excel macro provided by BioRad). An endogenous control, Glyceraldehyde 3-phosphate dehydrogenase (GAPDH) was employed as a normalization control. PLGA served as the vehicle control.

Immunoblotting

In this experiment, 2×10^6 cells were plated on 100 mm plates and incubated overnight for cellular attachment. Cells were then treated with 10 nM PTX or PPNPs for 48 h.

Then, cells were washed twice with 1X PBS, and 300µL of SDS buffer (Santa Cruz Biotechnology, Santa Cruz, CA) containing 10 µL/ml each of protease/phosphatase inhibitors and EDTA added to each plate to lyse cells. Cell lysates were then collected by scraping cells with a cell scraper into 1.5 ml centrifuge tubes. Lysates were subsequently sonicated for 30–40 s and spun at 15,000 rpm at 4 °C for 15min and supernatant collected. All steps were carried out on ice. Next, the Bradford Assay was employed to determine the quantities of protein concentration in each sample. 20 µg of protein from each treatment group was loaded and differentiated by 4–20% SDS-PAGE gel electrophoresis at 100 V for 80 min. Separated proteins were then be transferred onto a poly (vinylidene difluoride) (PVDF) membrane and electrophoresed at 100 V for 80 min. The blots were then blocked with 5% non-fat milk in Tris buffered Saline with Tween 20 (TBS-T) at room temperature for 1 hour and subsequently incubated with specific primary antibodies at 4 °C for 24 h. Antibodies included components of the Sonic Hedgehog Pathway including Sonic hedgehog (SHH), Patched 1 (PTCH1), and Glioma-Associated Oncogene Homolog-1 (GLi-1) transcription factor. After incubation, the blots were washed three times with TBS-T for 5 min each and incubated with antirabbit/mouse secondary antibodies for an hour at room temperature. To detect protein signals, blots were washed again, three times with TBS-T for 15 min (5 min per wash), and then the blots were soaked in a Lumi Light reagent (Roche, Nutley, NJ) and visualized with a gel doc machine (Bio-Rad, Hercules, CA).

Statistical Methods

Statistical analysis was determined by using an unpaired, two tailed student's t-test. The results were considered significant (*) if $P < 0.05$. All graphs were generated using GraphPad Prism5 software. Quantification of protein expression was done using GelQuant.NET from Biochemlabsolutions.com.

Results

PPNPs Formulation Efficiently Inhibits Expression of Components of The Sonic Hedgehog Signaling Pathway in PanCa cells

SHH signaling pathway is a critical pathway that modulates key developmental processes such as growth and multicellular embryonic patterns. Defects in signal transduction of this pathway has been implicated in birth defects, tissue regeneration, stem cell renewal and carcinogenesis (Choudhry et al.). Recent studies have shown that SHH signaling facilitates PanCa progression. Additionally, paracrine SHH signaling is vital in the tumor-stroma crosstalk interactions that establishes a desmoplastic PanCa TME ((Bailey et al.). First, SHH ligand binds to PTCH1, activates the Smoothened (SMO) transducer protein, and subsequently upregulating activity of downstream factors such as the GLi family of transcription factors. This cascade modulates target gene expression to increase cell proliferation, survival, and angiogenesis (Choudhry et al.). In this study, it was observed that PPNPs significantly downregulated gene expression of key components of SHH pathway including SHH (Figure 7-1, i), GLi-1 (Figure 7-1, ii) and PTCH1 (Figure 7-1, iii) more efficiently compared to free PTX in both Panc-1 (Figure 7-1, A) and HPAF-II cell lines (Figure 7-1, B). Further, PPNPs inhibited protein expression of these components downstream of these genes in both Panc-1 (Figure 7-2, A) and HPAF-II (Figure 7-2, B) cell lines in a superior manner compared to free PTX.

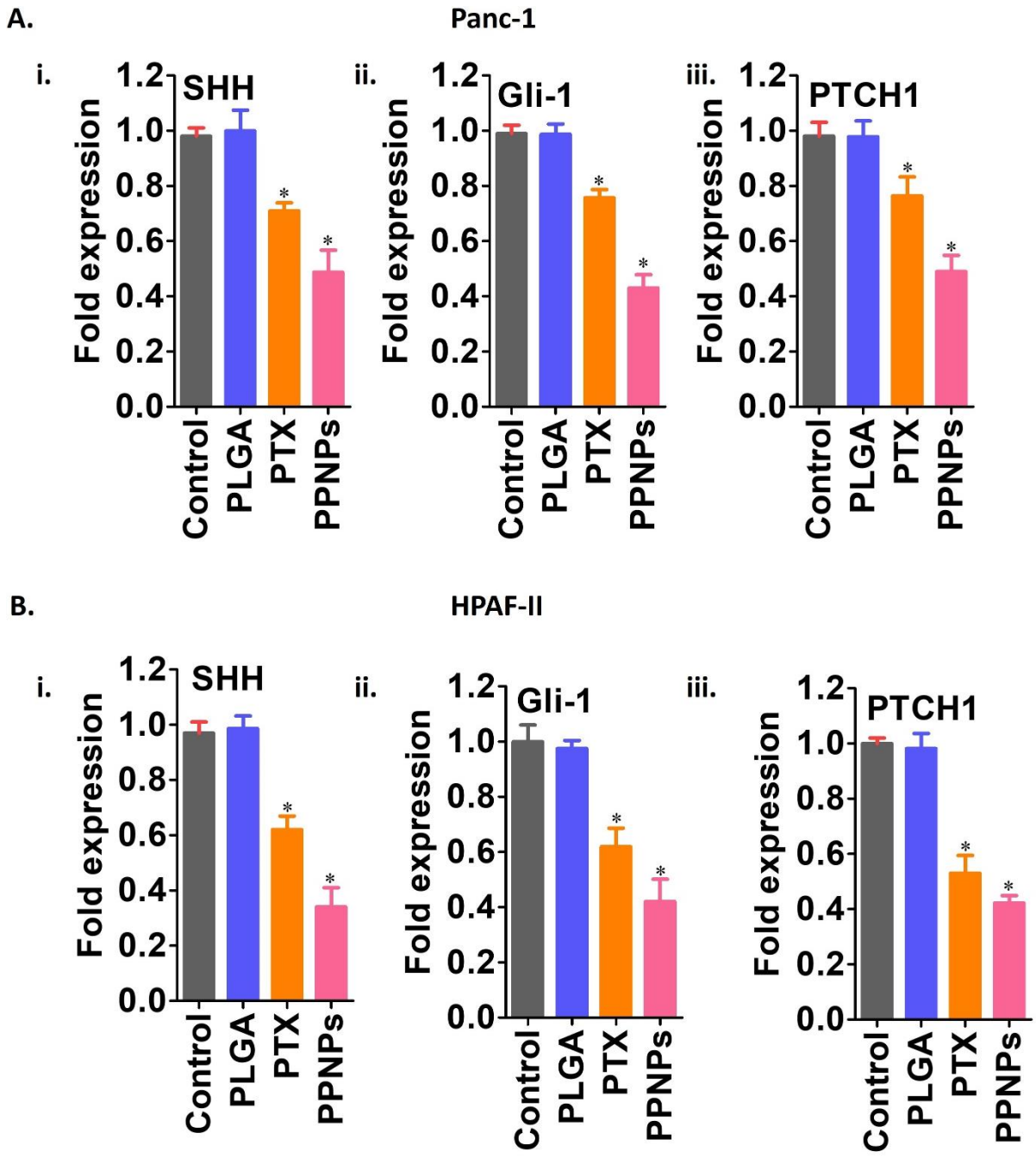

Figure 7-1. PPNPs formulation efficiently inhibits gene expression of components of the Sonic Hedgehog signaling pathway. qRT-PCR analysis of SHH (i), Gli-1(ii) and PTCH1 (iii) in Panc-1 (A) and HPAF-II (B) cells.

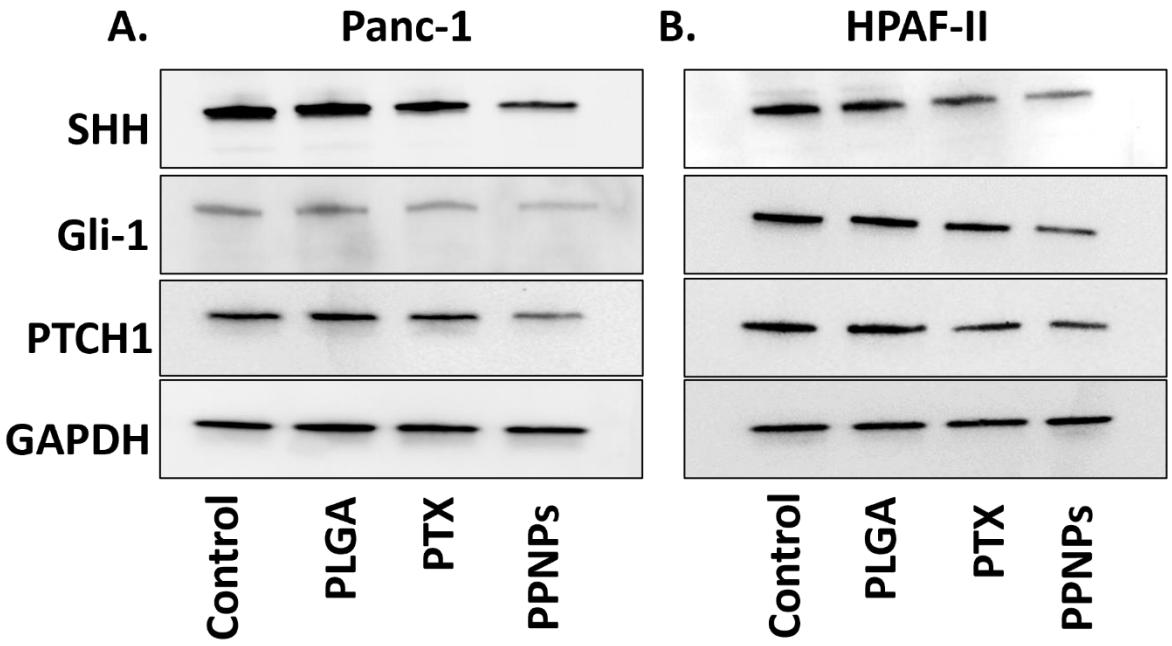

Figure 7-2**.** PPNPs formulation sufficiently inhibits protein expression of components of the Sonic Hedgehog signaling pathway. Western Blot analysis of SHH markers in Panc-1 (A) and HPAF-II (B) cell lines as determined by Western Blot Analysis.

CHAPTER VIII

DETERMINATION OF EFFECT OF PPNPs ON ANTI-CANCER ACTIVITY OF GEMCITABINE IN PANCREATIC CANCER CELLS

Materials and Methods

Cell Viability Assay

In the cell viability assay, PanCa cell lines (Panc-1 and HPAF-II) were seeded at 1×10^5 cells/well density in 12-well plates and incubated at 37°C for 24 h to facilitate cell attachment. After incubation, the cells were treated with 10 nM concentrations of either free PTX or PPNPs and combinations of either drug with 100 nM GEM for 48 h. DMSO served as control and Poly (lactide-*co*-glycolide) (PLGA) without the drug were used as vehicle controls. After 48 h, cells were imaged under an optical microscope to observe treatment effects. Images were captured with an Olympus microscope (Olympus, Center Valley, PA). Next, spent media was aspirated and cells washed twice with 500 µL of 1X PBS. To detach cells, 200 µL of 0.25% Trypsin reagent was added to each well, and plates were incubated for 3-5 min at 37°C. Next, 800 µL of appropriate media was mixed with each well to stop trypsinization. 10 µL of cell suspension was then mixed with 10 µL 0.4% Trypan Blue stain (Thermofisher Scientific). Then, 10 µL of trypan-blue and cell suspension mixture was pipetted into Countess Cell Counting Chamber Slide (Thermofisher Scientific). Changes in cell viability for each cell line was then recorded as live cell counts using Invitrogen Cell Countess machine.

Colony Forming Assay

PanCa cell lines (Panc-1, HPAF-II, AsPC-1, MIA PaCa-2) were seeded at the density of 500 cells/well in 12-well plates and incubated at 37°C with 5% CO_2 for 24 h to facilitate cell attachment. Next, the cells were treated with 2.5 nM concentrations of either free PTX or PPNPs and combinations of either drug with 5 nM GEM. Plates were then subsequently incubated for 14–16 days. Poly (lactide-*co*-glycolide) (PLGA) without drug were used as vehicle controls. During plate termination, plates were washed twice with 1X PBS to remove dead colonies, fixed with ice-cold methanol (MeOH), stained with 0.5% crystal violet in 25% methanol, and washed with running distilled water. Plates were then air-dried and visualized with a gel doc (Bio-Rad, Hercules, CA). Colonies were counted using ImageJ (Image J software, NIH USA), and each experiment conducted in triplicates for accuracy of results.

Boyden Chamber Cell Migration Assay

Cell migration assay was performed in a 96 well format HTS transwell plate from Corning. All PanCa cell lines utilized (Panc-1, HPAF-II, AsPC-1, and MIA PaCA-2) were serum starved. Next day, 30,000 cells/well density of each cell line were seeded in the upper chambers containing serum free culture medium with 2.5 nM concentration each of PTX and PPNPs treatment as well as combination treatment of either drug with 5nM GEM was prepared in serum-free media accordingly. Total volume of cell suspension, drug volume and serum-free media was 100 µL in each of the upper chambers. Seeded cells were then urged to migrate towards the lower chamber containing 250 µL media enriched with 10% FBS for 24 h. At the end of the indicated treatment period, cells were washed twice with 100 µL PBS and subsequently fixed with 100 µL 4% paraformaldehyde prepared in PBS for 20 min at room temperature and stained with crystal violet for 20 min.

Plates were then washed with running distilled water to remove any excess stains. Cells that failed to migrate from the upper chamber were completely removed by cotton swab while wet, and this was carefully done to prevent swab from touching membrane of upper chamber. Plates were then air-dried overnight, and migrated cells that were stuck on the membrane of the upper chamber were observed/ imaged by using light microscope (EVOS 7000) at 10X magnification. Each experiment was performed in triplicates for reproducibility of results.

Boyden Chamber Matrigel Cell Invasion Assay

For invasion assay, we used BD Bio coat Matrigel Invasion Chambers 24 transwell format (BD Biosciences). For this assay, PanCa cells to be seeded (Panc-1, HPAF-II, AsPC-1, and MIA PaCA-2) were serum-starved overnight. The next day, invasion chambers/inserts were filled with 500 µL serum free culture medium for 120 min at 37º C to activate the membrane of the inserts. 30,000 cells/well of each cell line was plated the next day in 500 uL serum-free media into the upper chamber/insert after activation. The lower wells were filled with 500 µL serum free media and the whole plate containing both upper and lower chambers was incubated at 37º C for 24 h for cellular attachment. Next day, PPNPs treatment at 2.5 nM concentration, PTX 2.5 nM as well as combination treatment of either drug with 5 nM GEM prepared in 500 µL serum free media were administered to the seeded cells in the upper chambers, and the serum free media in lower wells was replaced with appropriate media enriched with 10% FBS. Cells were now urged to invade the Matrigel towards FBS gradient in the lower chamber for the next 24 h. After 24 h, the cells were washed twice with 500 µL PBS and fixed with 500 µL of 4% paraformaldehyde for 20 min at room temperature. Next, fixed cells were stained with 0.5% crystal violet for another 20 min, washed with running distilled water, and air dried.

Cells stuck on the membrane of the chamber/insert (invaded cells) were imaged at 10X magnification by using a light microscope (EVOS 7000 Microscope).

Statistical Methods

Quantitative data were presented as mean ± standard error (SEM) in this study. Statistical analyses were conducted by using one-way ANOVA. The results are considered significant if p-values < 0.05 ($\alpha = 0.05$). All graphs were generated using GraphPad Prism (5.03, GraphPad Software, Inc., La Jolla, CA, USA).

Results

PPNPs Efficiently Potentiate GEM Activity to Inhibit Cell Viability of PanCa Cells

A potent anti-cancer agent actively targets survival mechanisms employed by cancer cells to decrease cell viability and cellular proliferation of these cells, eventually killing the cells. Failure of single agent drugs to effectively eliminate cancer cells has necessitated development of combination therapies that can exert synergistic anti-cancer effects on cancer cells and yield improved clinical outcomes, especially for PanCa. GEM is the current gold standard of care for PanCa therapy but the acquisition of GEM resistance by PanCa cells, especially PDAC cells also presents a therapeutic challenge. Numerous studies have investigated the potency of PTX and GEM as a combination module to address chemoresistance and improve therapeutic outcomes in clinical settings, with encouraging results but patients barely record a massively improved OS rate. PPNPs formulation is equipped with a unique, Pluronic F127 polymer that has been demonstrated to chemo sensitize PanCa TME to GEM therapy.

As such, we sought to investigate the efficiency of PPNPs in potentiating GEM activity in PanCa cells. Our findings demonstrated that treatment of PanCa cells with PPNPs alone and with GEM as a combination module effectively decreased cellular viability of Panc-1 (Figure 8-1, A)

and HPAF-II (Figure 8-1, B), which are known GEM-resistant PanCa cell lines, in a superior manner compared to PTX alone and PTX-GEM combinations at the same concentration. DMSO served as a control and PLGA was used as a vehicle control.

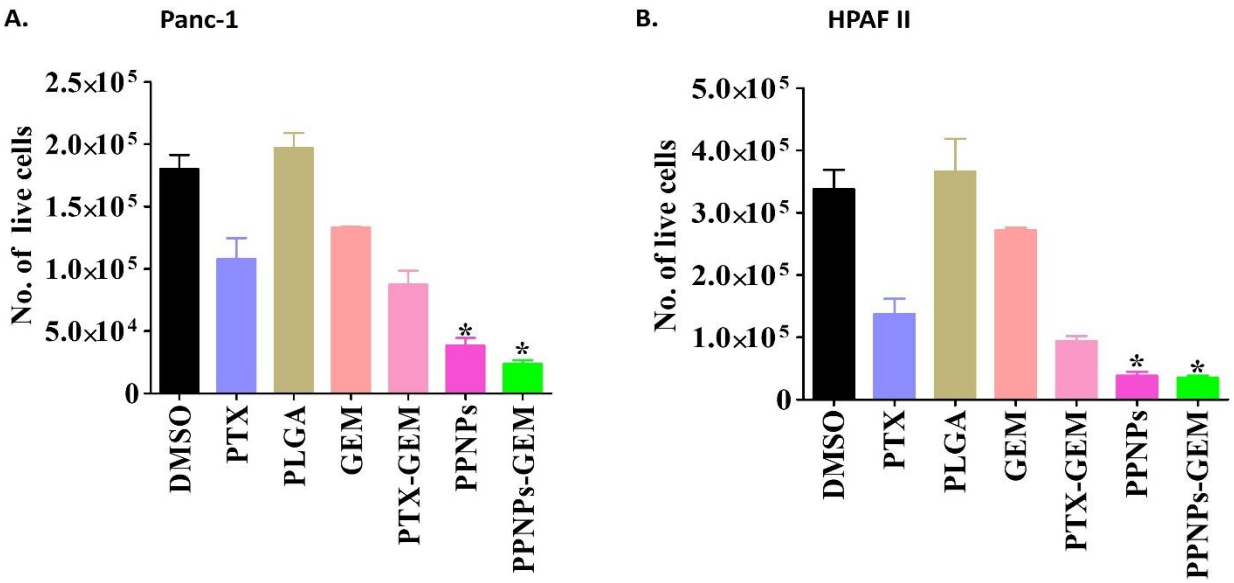

Figure 8-1. Effect of PPNPs alone and in combination with GEM on cell viability of PanCa cells. Average live cell counts of Panc-1 (A) and HPAF-II (B). Values in bar graph represent mean ± SEM of 3 wells. Significant values = *$p < 0.05$

PPNPs-GEM Combination Suppresses Clonogenic Potential of PanCa Cells

Our findings also demonstrated that PPNPs alone and combination regimen of PPNPs and GEM significantly decreased colony forming abilities of Panc-1 (Figure 8-2, A) and HPAF-II (Figure 8-2, B) cell lines compared to PTX alone and PTX-GEM combinations. Statistical analysis confirmed that PPNPs-GEM drastically reduced the clonogenic potential of Panc-1 (Figure 8-2, i) and HPAF-II (Figure 8-2, ii) cell lines more efficiently than PTX-GEM combinations.

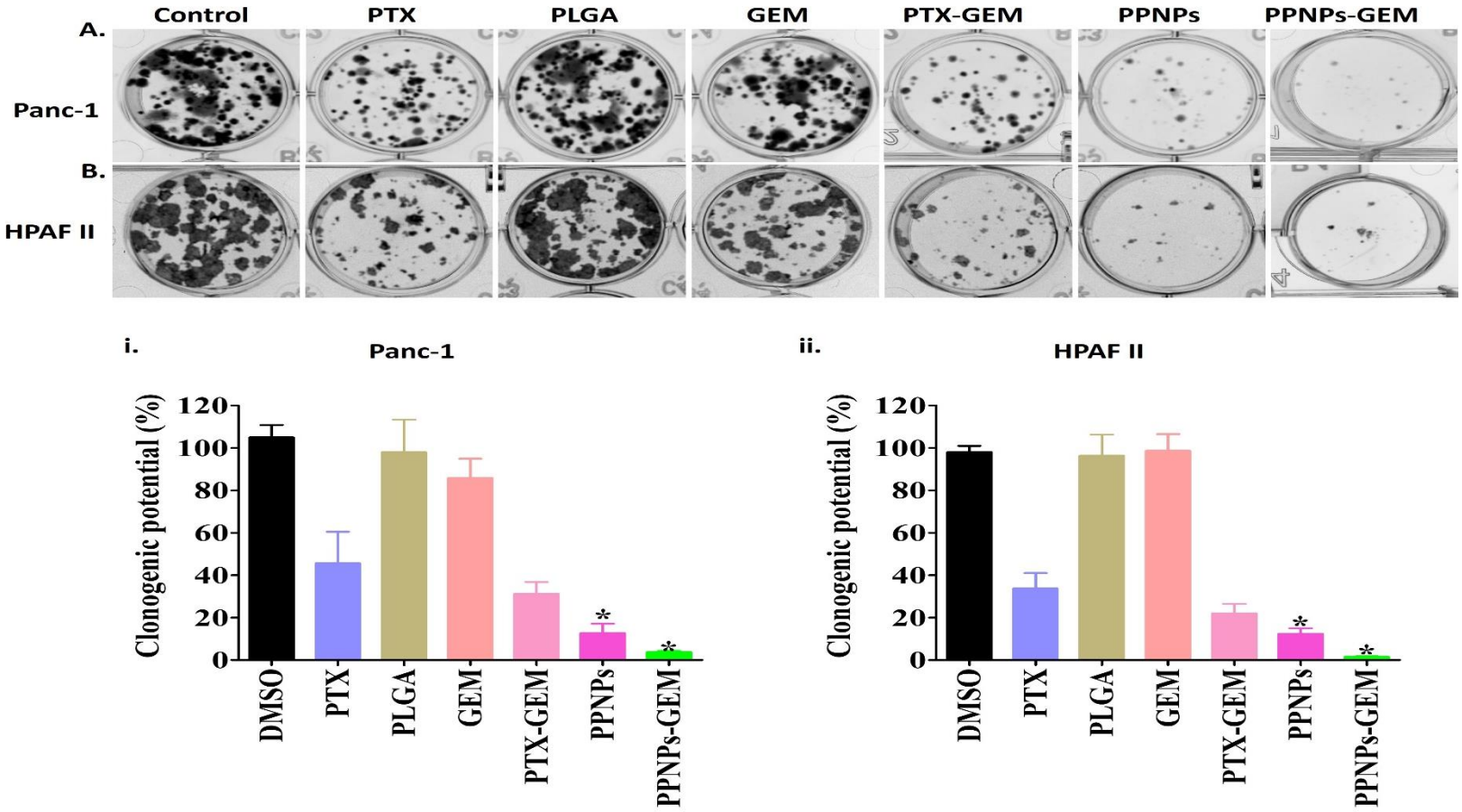

Figure 8-2. Effect of PPNPs alone and in combination with GEM on clonogenic potential of PanCa cells. Representative colony images of PPNPs and PPNPs-GEM treatment of Panc-1 (A) and HPAF-II (B). Average colony counts of Panc-1 (i) and HPAF-II (ii). Values in bar graph represent mean ± SEM of 3 wells. Significant values = *$p < 0.05$

PPNPs-GEM Combination Effectively Inhibits Migratory Potential of PanCa Cells

The loss of an epithelial phenotype and the concurrent acquisition of a mesenchymal phenotype via Epithelial-Mesenchymal Transition (EMT) regulates metastatic propensities of PanCa cells that enable them to migrate from local tumor sites and the TME and subsequently invade neighboring and distal systemic tissues to establish disease progression, leading to advanced disease. GEM-resistant PanCa cells exert enhanced EMT properties and chemoresistance. As such, we investigated the ability of PPNPs to suppress migration of PanCa cells. It was observed that PPNPs alone as well as combination regimen of PPNPs and GEM (PPNPs-GEM) effectively suppressed migratory properties of Panc-1 (Figure 8-3, A) and HPAF-II (Figure 8-3, B) much better than free PTX and PTX-GEM combinations. The average counts of migrated cells after treatment confirmed that PPNPs and PPNPs-GEM treatment significantly reduced the number of migrated cells compared to free PTX and PTX-GEM combinations in both Panc-1 (Figure 8-3, i) and HPAF-II (Figure 8-3, ii) cell lines.

PPNPs-GEM Combination Effectively Inhibits Invasive Potential of PanCa Cells

Our results also showed that treatment of PanCa cell lines with PPNPs and PPNPs-GEM combinations had a superior anti-cancer effect on the invasive potential of Panc-1 (Figure 8-4, A) and HPAF-II (Figure 8-4, B) compared to free PTX and PTX-GEM combinations. Statistical analysis demonstrated that PPNPs and PPNPs-GEM treatment had a highly significant impact on the invasive potential of Panc-1 (Figure 8-4, i) and HPAF-II (Figure 8-4, ii) cell lines, much better than PTX and PTX-GEM combinations, respectively.

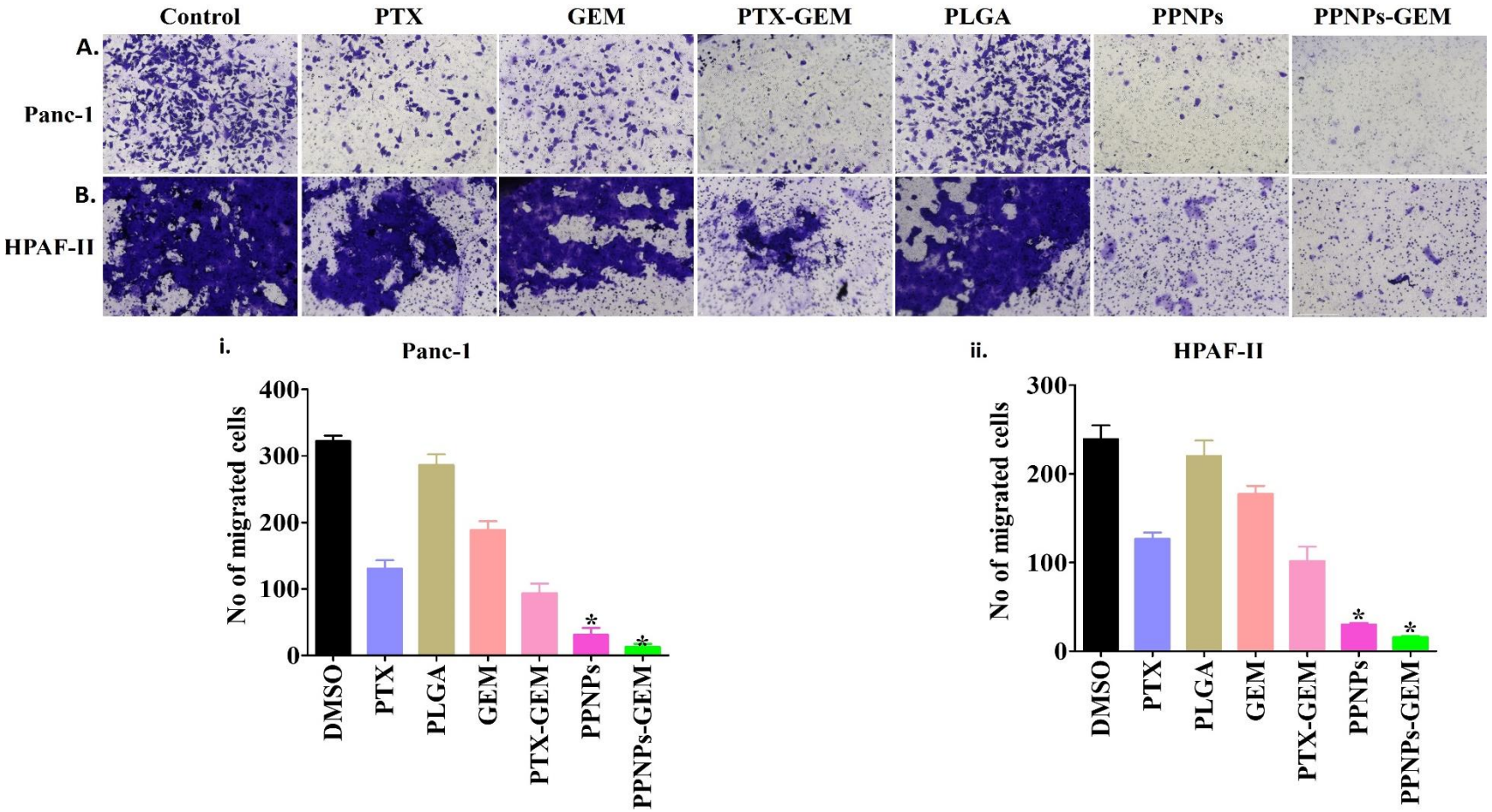

Figure 8-3. Effect of PPNPs alone and in combination with GEM on migratory potential of PanCa cells. Representative images of PPNPs and PPNPs-GEM combination treatments of Panc-1 (A) and HPAF-II (B) cells. Average cell counts of Panc-1 (i) and HPAF-II (ii). Values in bar graph represent mean ± SEM of 3 wells. Significant values = *$p < 0.05$

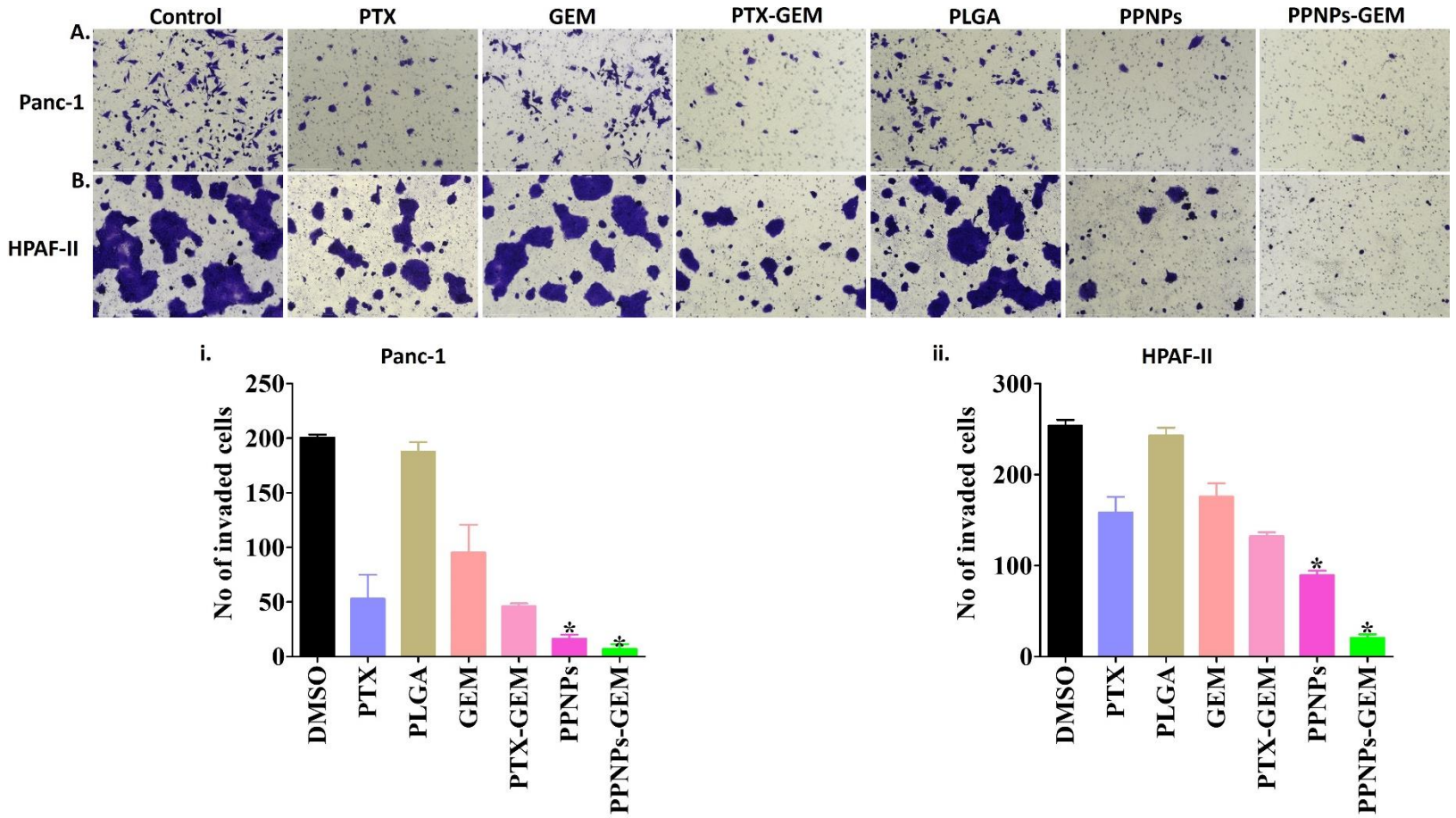

Figure 8-4. Effect of PPNPs alone and in combination with GEM on invasive potential of PanCa cells.

Representative images of PPNPs and PPNPs-GEM combination treatments of Panc-1 (A) and HPAF-II (B) cells. Average cell counts of Panc-1 (i) and HPAF-II (ii). Values in bar graph represent mean ± SEM of 3 wells. Significant values = *$p < 0.05$

CHAPTER IX

DETERMINATION OF THE EFFECT OF PPNPs ALONE AND IN COMBINATION WITH GEMCITABINE ON SHH AND GLI-1 AND THE KEY MOLECULES INVOLVED IN PANCREATIC DESMOPLASIA

Materials and Methods

Immunoblotting

In this experiment, 2×10^6 cells were plated on 100 mm plates and incubated overnight for cellular attachment. Cells were then treated with 10 nM PTX or PPNPs and combinations of either drug with 100 nM GEM for 48 h. Then, cells were washed twice with 1X PBS, and 300µL of SDS buffer (Santa Cruz Biotechnology, Santa Cruz, CA) containing 10 µL/ml each of protease/phosphatase inhibitors and EDTA added to each plate to lyse cells. Cell lysates were then collected by scraping cells with a cell scraper into 1.5ml centrifuge tubes. Lysates were subsequently sonicated for 30–40 s and spun at 15,000 rpm at 4 °C for 15 min and supernatant collected. All steps were carried out on ice. Next, the Bradford Assay was employed to determine the quantities of protein concentration in each sample. 20 µg of protein from each treatment group was loaded and differentiated by 4–20% SDS-PAGE gel electrophoresis at 100 V for 80 min. Separated proteins were then transferred onto a poly vinylidene difluoride (PVDF) membrane and electrophoresed at 100 V for 80 min.

The blots were then blocked with 5% non-fat milk in TBS-T at room temperature for 1 hour and subsequently incubated with specific primary antibodies at 4 °C for 24 h. Antibodies included components of the Sonic Hedgehog Pathway including SHH and Gli-1 as well as key desmoplasia factors such as fibroblast marker, α-smooth muscle actin (α-SMA), anti-apoptotic proteins, B-cell lymphoma-extra Large (Bcl-xL) and Cleaved PARP. After incubation, the blots were washed three times with TBS-T for 5 min each and incubated with antirabbit/mouse secondary antibodies for an hour at room temperature. To detect protein signals, blots were washed again, three times with TBS-T for 15 min (5 min per wash), and then the blots were soaked in a Lumi Light reagent (Roche, Nutley, NJ) and visualized with a gel doc machine (Bio-Rad, Hercules, CA). GAPDH served as the loading control.

Statistical Methods

Statistical analysis was determined by using an unpaired, two tailed student's t-test. The results were considered significant (*) if $P < 0.05$. All graphs were generated using GraphPad Prism5 software. Quantification of protein expression was done using GelQuant.NET from Biochemlabsolutions.com.

Results

PPNPs Regulate Expression of Key Molecules and Signaling Pathways Involved In Establishing Pancreatic Desmoplasia

The presence of a desmoplastic TME impedes drug delivery because of high interstitial fluid pressure and can eventually result in off-target toxicities and ineffective treatment strategies. The SHH signaling pathway has been largely implicated in establishing a dense, fibrotic TME that re-programs vascularization in the pancreatic TME and creates an

immunosuppressive environment. As such, we sought to investigate the ability of PPNPs and GEM combination to target key molecules and the SHH pathway to reprogram the pancreatic TME and chemo sensitize it to GEM therapy. Our results demonstrated that PPNPs-GEM sufficiently downregulated expression of key components of the SHH pathway such as SHH and Gli-1 in both Panc-1 (Figure 9-1, A) and HPAF-II (Figure 9-1, B) and altered expression of desmoplasia factors such as α-SMA, Bcl-xL and Cleaved PARP in Panc-1 (Figure 9-1, C) more effectively than PTX-GEM combinations.

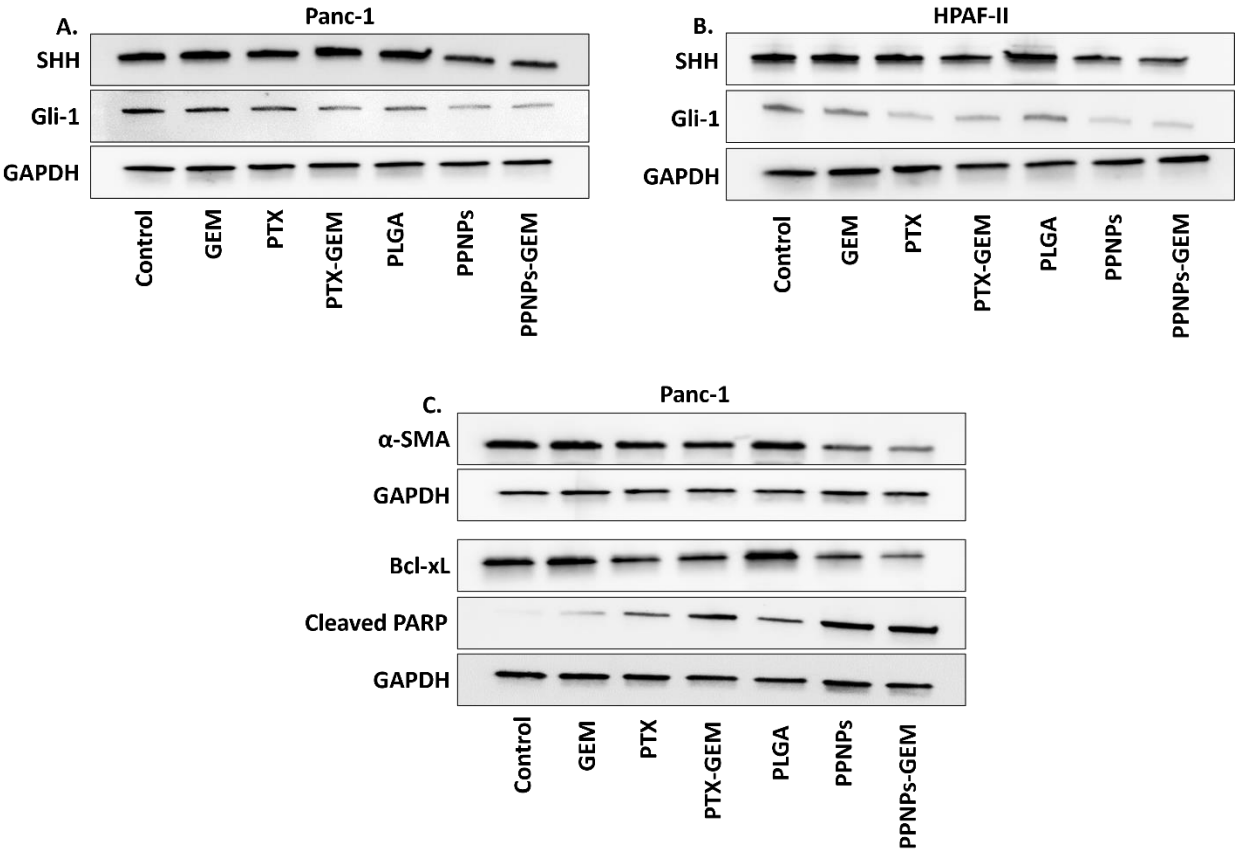

Figure 9-1. Effect of PPNPs alone and in combination with GEM on SHH and Gli-1 and the key molecules involved in pancreatic desmoplasia. Western blot analysis of PPNPs-GEM combination on the expression of components of SHH pathway in Panc-1 (A) and HPAF-II (B), and key desmoplasia factors in Panc-1 (C).

CHAPTER X

DETERMINATION OF THE EFFECT OF PPNPs ON M1/M2 POLARISATION IN RAW 264.7 CELLS

Materials and Methods

Quantitative Real Time-Polymerase Chain Reaction

To assess the relative gene expression activity of murine macrophages treated with PPNPs and PPNPs-GEM combinations, 1×10^6 RAW 264.7 cells were plated on 100 mm plates and incubated overnight for cellular attachment. Then, cells were treated with 10 nM concentration of PTX and PPNPs and combinations of either drug with 100 nM GEM and incubated for 48 h. Next, the adherent cells were collected, and the total RNA extracted with the Qiagen RNeasy kit (Qiagen Inc., Valencia, CA, USA). Reverse transcription was performed with the High-Capacity RNA to cDNA kit and amplified with SYBR Green PCR master mix (both from Applied Biosystems) for cDNA synthesis. qRT-PCR \was performed to determine the expression of M1/ M2 markers such as Cluster of differentiation 206 (CD206), Arginase-1 (Arg-1), inducible Nitric Oxide Synthase (iNOS), Programmed Death receptor -1 (PD-1), Programmed Death receptor - Ligand 1 (PD-L1), Interleukin-6 (IL-6), Interleukin-10 (IL-10) and Signal Transducer and Activator of Transcription-3 (STAT-3).

Each reaction was performed in triplicates with a MyiQ single-color real-time PCR thermocycler and analyzed with GeneX (Microsoft Excel macro provided by BioRad). An endogenous control, Glyceraldehyde 3-phosphate dehydrogenase (GAPDH) was employed as a normalization control. PLGA served as the vehicle control.

Immunoblotting

In this experiment, 2×10^6 RAW 264.7 cells were plated on 100 mm plates and incubated overnight for cellular attachment. Cells were then treated with 10 nM PTX or PPNPs and combinations of either drug with 100 nM GEM for 48 h. Then, cells were washed twice with 1X PBS, and 300µL of SDS buffer (Santa Cruz Biotechnology, Santa Cruz, CA) containing 10 µL/ml each of protease/phosphatase inhibitors and EDTA added to each plate to lyse cells. Cell lysates were then collected by scraping cells with a cell scraper into 1.5ml centrifuge tubes. Lysates were subsequently sonicated for 30–40 s and spun at 15,000 rpm at 4 °C for 15 min and supernatant collected. All steps were carried out on ice. Next, the Bradford Assay was employed to determine the quantities of protein concentration in each sample. 20 µg of protein from each treatment group was loaded and differentiated by 4–20% SDS-PAGE gel electrophoresis at 100 V for 80 min. Separated proteins were then be transferred onto a poly (vinylidene difluoride) (PVDF) membrane and electrophoresed at 100 V for 80 min. The blots were then blocked with 5% non-fat milk in Tris buffered Saline with Tween 20 (TBS-T) at room temperature for 1 hour and subsequently incubated with specific primary antibodies at 4 °C for 24 h. Western blot analysis was performed to determine the protein level of iNOS, Arginase-1, CD206, pStat3. GAPDH was used as loading control. After incubation, the blots were washed three times with TBS-T for 5 min each and incubated with antirabbit/mouse secondary antibodies for an hour at room temperature.

To detect protein signals, blots were washed again, three times with TBS-T for 15 min (5 min per wash), and then the blots were soaked in a Lumi Light reagent (Roche, Nutley, NJ) and visualized with a gel doc machine (Bio-Rad, Hercules, CA).

Statistical Methods

Statistical analysis was determined by using an unpaired, two tailed student's t-test. The results were considered significant (*) if $P < 0.05$. All graphs were generated using GraphPad Prism5 software. Quantification of protein expression was done using GelQuant.NET from Biochemlabsolutions.com.

Results

PPNPs Reprogram Tumor-Associated Macrophages to an M1 Profile

A critical component of host immune defense system is macrophages which release inflammatory cytokines upon pathogenic invasion to eliminate harmful cells. However, in most types of cancer such as PanCa, abnormalities in the host immune defense programming mediated by oncogenic cells lead to interleukin-4 (IL-4) induced polarization of M1 pro-inflammatory macrophages to M2 immunosuppressive macrophages which facilitate tumor development and progression. This is a key transformation event that creates immunosuppressive conditions in the TME and facilitates metastasis. As such, we investigated the ability of PPNPs to repolarize Tumor-Associated Macrophages to an M1 profile. Gene expression analysis by qRT-PCR demonstrated that PPNPs effectively decreased expression of M2 markers and polarization components such as Arg-1, IL-10, STAT-3, PD-1, PD-L1 and CD206 (Figure 10-1. A-F respectively), in a superior manner compared to free PTX and vehicle control (PLGA).

PPNPs also concurrently upregulated expression of IL-6 and iNOS (Figure 10-2, G-H respectively) which are key markers of M1 macrophages, more efficiently than free PTX, indicating the potency of PPNPs in maintaining a proinflammatory phenotype of macrophages and inhibiting polarization of M1/M2 macrophages. IL-4 served as a marker of polarization. Further, PPNPs effectively downregulated protein expression of M2 marker proteins such as CD206, Arg-1, and pSTAT-3 and increased expression of M1 marker iNOS relative to free PTX and vehicle and IL-4 controls (Figure 10-2). This emphasizes the activity of PPNPs in suppressing M1/M2 macrophage polarization and promoting inflammation.

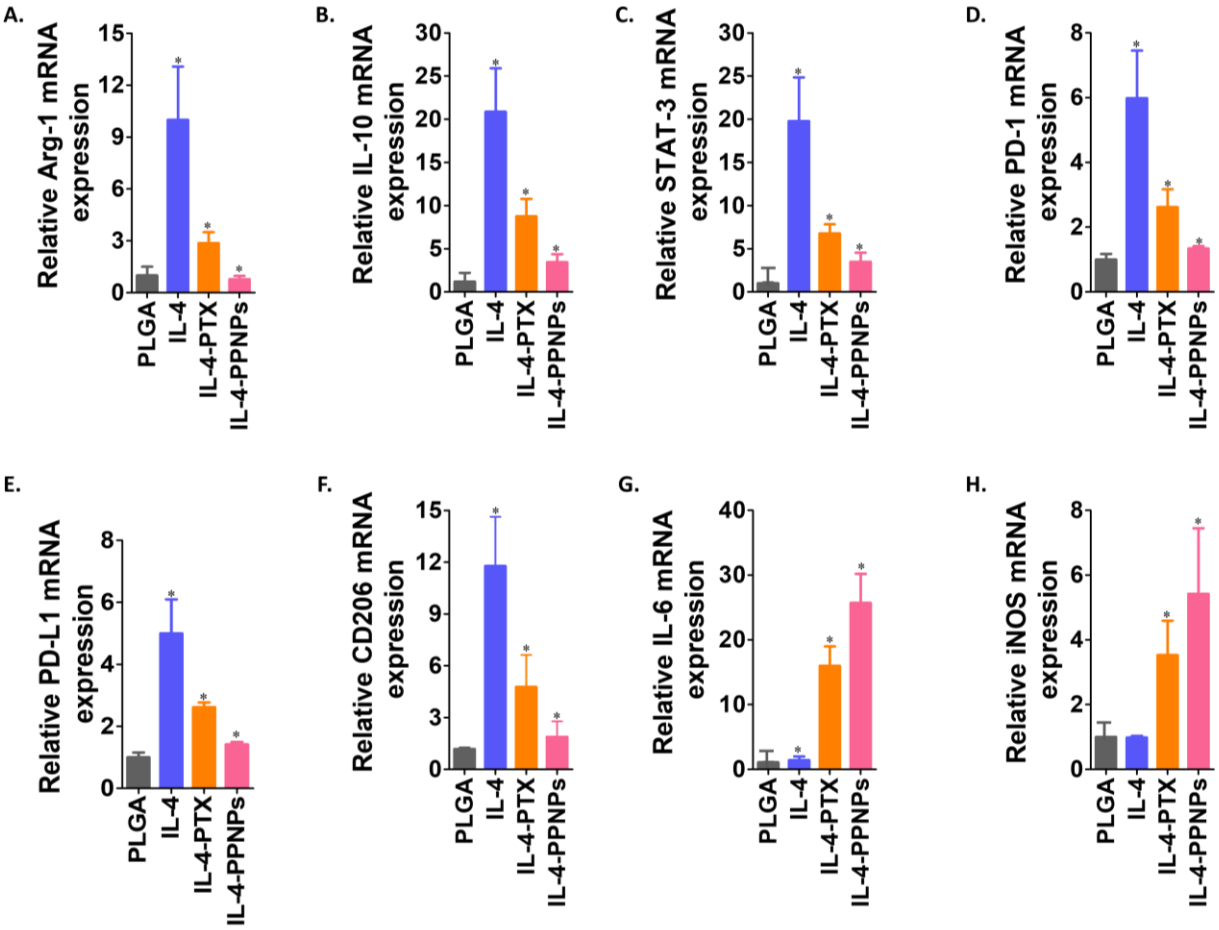

Figure 10-1. qRT-PCR analysis of effect of PPNPs on gene expression of M1/M2 polarization markers. Analysis of markers such as Arg-1 (A), IL-10 (B), STAT-3 (C), PD-1 (D), PD-L1 (E), CD206 (F), IL-6 (G) and iNOS (H). Values in bar graph represent mean ± SEM of 3 wells. Significant values = *$p < 0.05$

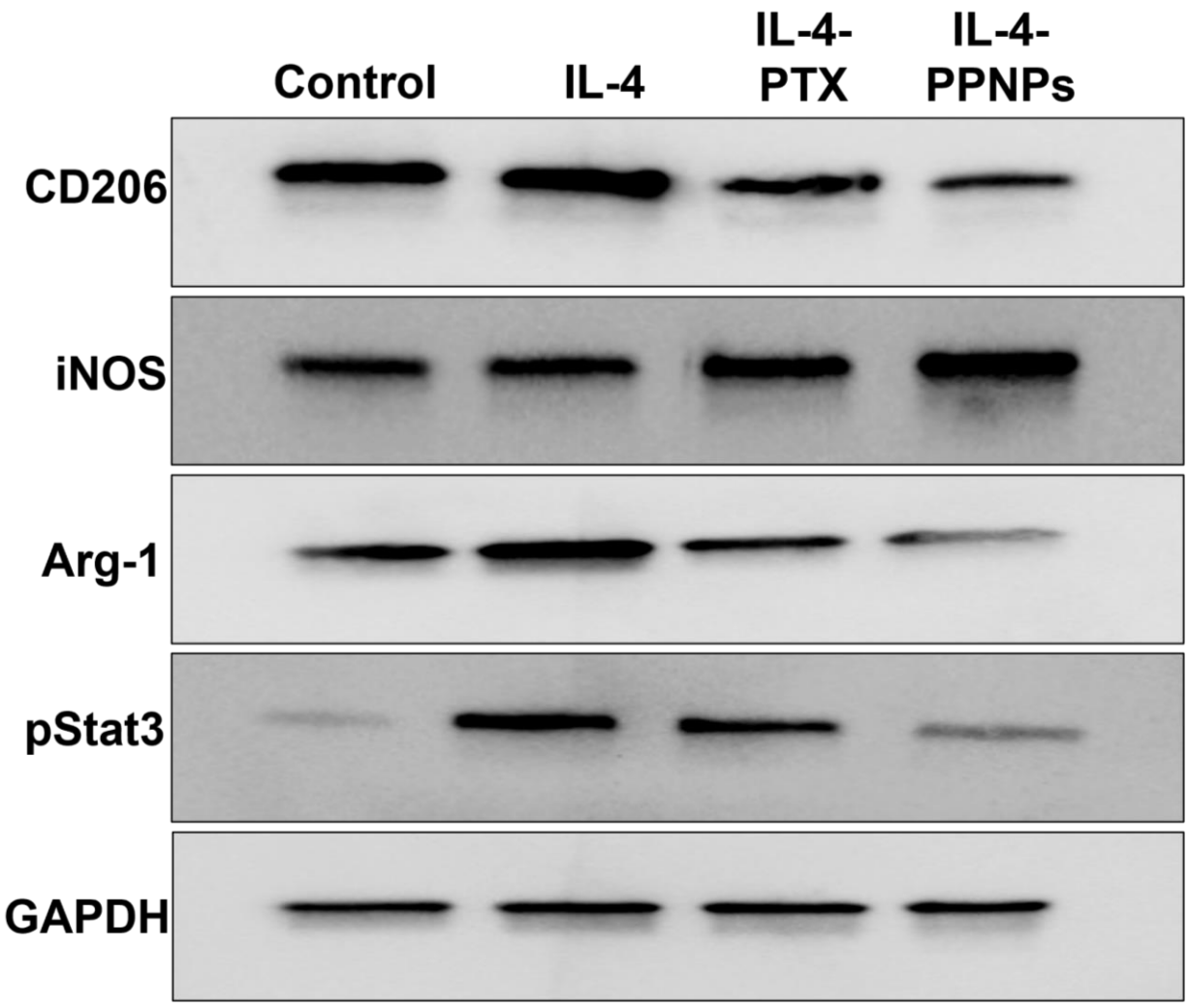

Figure 10-2. Western blot analysis of effect of PPNPs on M1/M2 polarization markers. Analysis of protein expression of select M1 and M2 markers. GAPDH served as a loading control

CHAPTER XI

DISCUSSION

PanCa remains a lethal disease in the U.S because of the high disease burden and ineffective therapeutic options (Siegel RL). Only 10-20 out of 100 patients suffering from localized disease are eligible for surgery, and moreover, chances of the disease recurring post-surgery are very high (Rawla, Sunkara and Gaduputi). This is because of a dense, hypoxic, desmoplastic stroma in the pancreatic TME, particularly in PDAC, that impede drug therapy via deregulation of drug transporters and elevation of interstitial fluid pressure to inhibit drug delivery and accumulation (Torphy, Zhu and Schulick; Christine Feig et al.). This has been the main reason why most current therapeutic drugs against PDAC yield dismal outcomes. PTX which has been utilized in breast (Perez), lung (Ramalingam and Belani) and ovarian cancer (Kampan et al.), has been applied in PDAC therapy with fairly positive outcomes, but only limited by its poor hemocompatibility and inefficient intracellular accumulation in tumor cells resulting in inadequate tumor elimination and local disease recurrence (Meng et al.). The current gold drug standard for PanCa chemotherapy, GEM, has also gradually lost its potency due to development of chemoresistance by the tumor cells in the pancreatic TME via deregulation of GEM uptake transporters (Farrell et al.).However, there has been a breakthrough in drug delivery recently with the advent of nanoscale drug delivery systems.

Nano formulations have been demonstrated to selectively accumulate in tumor tissues by exploiting the imperfections in the tumor vasculature, mainly through Enhanced Permeation and Retention (EPR) effect (Bertrand et al.; Acharya and Sahoo). The successes chalked by nano formulations such as Abraxane® in treating various cancers including PanCa (Palacio et al.; Cohen et al.; Kuwayama et al.), lend credence to the superiority of nanoscale drug delivery systems over free drugs in yielding better clinical outcomes. Additionally, nanoscale drug delivery systems have been demonstrated to enhance target specificity of drugs to circumvent drug resistance, and result in overall reduction in systemic toxicity (Markman et al.). However, a few limitations of nanoscale drug delivery systems such as Abraxane include short circulation half-life and development of chemoresistance (Pedziwiatr-Werbicka et al.). Moreover, Abraxane® has had limited clinical success in treating the highly desmoplastic and heterogenous pancreatic tumors. As such, we generated a next generation nano formulation of PTX (PPNPs) using F127 polymer, which has been demonstrated to reverse chemoresistance (Park, Park and Na), and primed it against PanCa using in vitro model systems. Synthesis and characterization of PPNPs was adapted with permission from Massey et. al. (Massey et al.). The nanoprecipitation method was employed in the generation of PPNPs. Data from DLS analysis showed PPNPs had a particle size of about 160nm on average, and had a negative zeta potential, which are optimal conditions for nanoscale drug delivery (Massey et al.). Moreover, data from FT-IR and XRD spectra demonstrated that PLGA peaks were identical to PPNPs peak, implying that PLGA remained unchanged by PTX loading (Massey et al.), but it is worthwhile to note that these spectra analysis only capture the overall composition and physical state of the nanoparticle.

Further, AFM data suggested no physical change in the properties of PLGA NPs after PTX encapsulation, as seen by identical modulus in PLGA and PPNPs (~ 12 GPa) (Figure 3-2, F). (Massey et al.). However, the bulk modulus of the other layers is unknown, meaning these results are semi-quantitative. Herein, we demonstrated that nanoencapsulation of PTX to generate PPNPs greatly enhanced the fundamental anti-tumor properties of PTX. PDAC arises when genetic precursor lesions to pancreatic tissues give rise to pancreatic intraepithelial neoplasia (PanIN), and PanIN progression through higher stages eventually result in PDAC formation (Polireddy and Chen). So far, K-Ras mutations are the most common mutations in PanCa and have been implicated in Stage 1 PanIN as pancreatic cells continually receive proliferative signals from hyperactive Ras (Polireddy and Chen). Our findings showed that treatment of PDAC cells with PPNPs significantly inhibited cellular proliferation and viability, suggesting nano encapsulated PTX inhibited microtubule depolymerization that is necessary for cellular trafficking and disrupted components of the K-Ras signaling cascade in PanCa cells. This is consistent with previous studies that have shown that intracellular trafficking of Ras proteins requires prenylation-dependent interplay between K-Ras and microtubules/tubulin, as deletion of the K-Ras poly-l-lysine region that binds microtubules, after cell treatment with PTX led to a loss of PTX-mediated mis localization of a fluorescent K-Ras fusion protein (Chen et al.). Hence, aberrant localization of Ras proteins would invariably disrupt intracellular proliferative signaling. Stage 3 PanIN which precedes PDAC development is characterized by disorganized structural architecture and nuclear atypia as TGF-β/SMAD-4 axis as well as EGF/EGFR interactions mediate loss of an epithelial phenotype and subsequent acquisition of a mesenchymal phenotype via type III EMT to support metastasis (Polireddy and Chen).

It has been shown that invasion and migration are two crucial mediators of metastatic cascades (Chambers, Groom and MacDonald). Metastatic malignant cells can then undergo extravasation at distant sites such as the liver and spleen and colonize these organs by re-gaining an epithelial phenotype at these secondary sites in the reverse process called Mesenchymal-to-Epithelial transition (MET). As such, our findings demonstrated that PPNPs efficiently enhanced anti-migratory properties of PTX in cancer cells by targeting the key molecular pathways that mediate EMT-MET and cells and subsequently decreased the clonogenic potential of these malignant cells in vitro. These results highlight the potential of PPNPs in effectively inhibiting EMT which is a crucial step in cancer metastasis. Our future studies would investigate the intricacies of this inhibition mechanism of PTX on EMT-MET components in PDAC. Also, attractive therapeutic targets for cancer therapy involve cell cycle arrest and apoptosis induction (Weinberg and Hanahan; Fisher), and several chemotherapeutic agents have chalked successes via targeting these mechanisms (J. Wang et al.; Karaca et al.). In fact, PTX has been demonstrated to mediate apoptosis induction and G2/M phase cell cycle arrest in various cancer cells by disrupting microtubule dynamics during cell division (Jiménez-Guerrero et al.), and our findings lend credence to this assertion as treatment of PanCa cells with PPNPs upregulated expression of pro-apoptotic proteins while concurrently suppressing protein expression of anti-apoptotic proteins. A major hallmark of PanCa, especially PDAC, is the TME which inhibits optimal drug delivery. Research has implicated crosstalk between PSCs and cancer cells as well as immune cells in establishing hypoxic, desmoplastic stroma in the TME with the SHH pathway playing a critical role in TME establishment (Polireddy and Chen). Therefore, we sought to investigate the influence of PPNPs in regulating components of the SHH pathway.

Interestingly, PPNPs significantly inhibited gene and protein expression of SHH components such as SHH ligand, Ptch-1, and Gli-1. These results suggest the superior anti-cancer potential of PPNPs compared to free PTX and presents PPNPs as a serious candidate for PanCa treatment. The next phase of our study investigated the influence of PPNPs in regulating pancreatic tumor immune components and sensitizing the fibrotic, chemo resistant pancreatic TME to GEM therapy. The disparate heterogeneity and cancer-stroma crosstalk within pancreatic tumors inhibit drug efficiency due to cellular mechanisms that deregulate drug transport, activation, and efficacy (Khan et al.). The rise of GEM resistance in pancreatic tumors poses a significant obstacle in PanCa therapy, leading to disease relapse. This is because drug transporters for GEM are deregulated in PanCa by PSCs and other immunosuppressive tumor components, limiting GEM intracellular accumulation and efficacy (Maeda et al.). Various combination regimens involving GEM have been churned out to avert this and combat PanCa but with barely enhanced survival rates (Von Hoff et al.). As such, we sought to investigate efficiency of PPNPs in potentiating GEM activity in pancreatic tumors. Our data obtained showed that combination treatment of PPNPs with GEM in PDAC cells showed significantly reduced cellular viability and colony formation ability of the cancer cells, as well as efficient inhibition of migratory and invasive potential of these cells. Moreover, PPNPs-GEM combination downregulated protein expression of key molecules involved in establishing pancreatic desmoplasia, such as α-SMA, which is a marker of activated PSCs (Polireddy and Chen), and SHH pathway components, suggesting that PPNPs may have positive therapeutic implications in modulating the pancreatic TME and chemo sensitizing it to GEM therapy.

Finally, our study also analyzed the effect of PPNPs on polarization of pro-inflammatory macrophages to immunosuppressive populations. Macrophages play critical roles in the inflammatory process and help combat systemic infections, However, in cancer cells, M1 macrophages which execute inflammatory attack against malignant cells and invaders are polarized to immunosuppressive M2 macrophages that deregulate the host immune response and aid in cancer progression. Interestingly, data from gene and protein expression analysis involving treatment of PDAC cells with PPNPs showed that PPNPs decreased expression of oncogenic M2 markers and maintained a pro-inflammatory phenotype of RAW 264.7 murine macrophages in vitro, emphasizing the positive influence of PPNPs on key immune components that regulate PanCa development and progression. Overall, these results present PPNPs as a highly attractive therapeutic modality in PanCa therapy, and the next phase of our study would involve active investigation of the molecular mechanisms and targeted delivery of PPNPs in pancreatic tumors using clinically relevant mouse model systems.

REFERENCES

Acharya, S., and S. K. Sahoo. "Plga Nanoparticles Containing Various Anticancer Agents and Tumour Delivery by Epr Effect." *Adv Drug Deliv Rev* 63.3 (2011): 170-83. Print.

Aglietta, Massimo, et al. "A Phase I Dose Escalation Trial of Tremelimumab (Cp-675,206) in Combination with Gemcitabine in Chemotherapy-Naive Patients with Metastatic Pancreatic Cancer." *Annals of oncology* 25.9 (2014): 1750-55. Print.

Allum, W. H. "Radioimmunolocalization of Tumours of the Pancreas and Biliary Tree." *Baillieres Clin Gastroenterol* 4.4 (1990): 853-67. Print.

Almoguera, C., et al. "Most Human Carcinomas of the Exocrine Pancreas Contain Mutant C-K-Ras Genes." *Cell* 53.4 (1988): 549-54. Print.

Anfray, Clément, et al. "Current Strategies to Target Tumor-Associated-Macrophages to Improve Anti-Tumor Immune Responses." *Cells* 9.1 (2019): 46. Print.

Ankeny, Jacob S, et al. "Circulating Tumor Cells Predict Occult Metastatic Disease and Prognosis in Pancreatic Cancer." *Annals of surgical oncology* 25.4 (2018): 1000-08. Print.

Apte, M. V., R. C. Pirola, and J. S. Wilson. "Pancreatic Stellate Cells: A Starring Role in Normal and Diseased Pancreas." *Front Physiol* 3 (2012): 344. Print.

Bailey, J. M., A. M. Mohr, and M. A. Hollingsworth. "Sonic Hedgehog Paracrine Signaling Regulates Metastasis and Lymphangiogenesis in Pancreatic Cancer." *Oncogene* 28.40 (2009): 3513-25. Print.

Bailey, J. M., et al. "Sonic Hedgehog Promotes Desmoplasia in Pancreatic Cancer." *Clin Cancer Res* 14.19 (2008): 5995-6004. Print.

Bertrand, N., et al. "Cancer Nanotechnology: The Impact of Passive and Active Targeting in the Era of Modern Cancer Biology." *Adv Drug Deliv Rev* 66 (2014): 2-25. Print.

Biankin, A. V., S. Piantadosi, and S. J. Hollingsworth. "Patient-Centric Trials for Therapeutic Development in Precision Oncology." *Nature* 526.7573 (2015): 361-70. Print.

Birnbaum, D. J., et al. "Prognostic Value of Pdl1 Expression in Pancreatic Cancer." *Oncotarget* 7.44 (2016): 71198-210. Print.

Borst, P. "Multidrug Resistance: A Solvable Problem?" *Ann Oncol* 10 Suppl 4 (1999): 162-4. Print.

Brower, V. "Checkpoint Blockade Immunotherapy for Cancer Comes of Age." *J Natl Cancer Inst* 107.3 (2015). Print.

Carbone, C., and D. Melisi. "Nf-Kappab as a Target for Pancreatic Cancer Therapy." *Expert Opin Ther Targets* 16 Suppl 2 (2012): S1-10. Print.

Cassetta, Luca, and Takanori Kitamura. "Targeting Tumor-Associated Macrophages as a Potential Strategy to Enhance the Response to Immune Checkpoint Inhibitors." *Frontiers in cell and developmental biology* (2018): 38. Print.Chambers, Ann F, Alan C Groom, and Ian C MacDonald. "Dissemination and Growth of Cancer Cells in Metastatic Sites." *Nature Reviews Cancer* 2.8 (2002): 563-72. Print.

Chen, Z., Z. Wang, and Z. Gu. "Bioinspired and Biomimetic Nanomedicines." *Acc Chem Res* 52.5 (2019): 1255-64. Print.

Chen, Zhui, et al. "The C-Terminal Polylysine Region and Methylation of K-Ras Are Critical for the Interaction between K-Ras and Microtubules." *Journal of Biological Chemistry* 275.52 (2000): 41251-57. Print.

Choudhry, Z., et al. "Sonic Hedgehog Signalling Pathway: A Complex Network." *Ann Neurosci* 21.1 (2014): 28-31. Print.

Cohen, Adam L, et al. "A Phase I Trial of Azacitidine and Nanoparticle Albumin Bound Paclitaxel in Patients with Advanced or Metastatic Solid Tumors." *Oncotarget* 8.32 (2017): 52413. Print.

Collins, M. A., et al. "Oncogenic Kras Is Required for Both the Initiation and Maintenance of Pancreatic Cancer in Mice." *J Clin Invest* 122.2 (2012): 639-53. Print.

Danhier, Fabienne, et al. "Plga-Based Nanoparticles: An Overview of Biomedical Applications." *Journal of controlled release* 161.2 (2012): 505-22. Print.

Di Marco, Mariacristina, et al. "Metastatic Pancreatic Cancer: Is Gemcitabine Still the Best Standard Treatment?" *Oncology reports* 23.5 (2010): 1183-92. Print.

Dinarvand, Rassoul, et al. "Polylactide-Co-Glycolide Nanoparticles for Controlled Delivery of Anticancer Agents." *International journal of nanomedicine* 6 (2011): 877. Print.

El-Zahaby, S. A., Y. S. R. Elnaggar, and O. Y. Abdallah. "Reviewing Two Decades of Nanomedicine Implementations in Targeted Treatment and Diagnosis of Pancreatic Cancer: An Emphasis on State of Art." *J Control Release* 293 (2019): 21-35. Print.

Elmore, S. "Apoptosis: A Review of Programmed Cell Death." *Toxicol Pathol* 35.4 (2007): 495-516. Print.

Ene-Obong, A., et al. "Activated Pancreatic Stellate Cells Sequester Cd8+ T Cells to Reduce Their Infiltration of the Juxtatumoral Compartment of Pancreatic Ductal Adenocarcinoma." *Gastroenterology* 145.5 (2013): 1121-32. Print.

Engbang, Jean Paul, et al. "Prognostic Factors and Survival of Laryngeal Cancer in Cameroon." *International Journal of Otolaryngology and Head & Neck Surgery* 10.01 (2021): 30. Print.

Engle, D. D., et al. "The Glycan Ca19-9 Promotes Pancreatitis and Pancreatic Cancer in Mice." *Science* 364.6446 (2019): 1156-62. Print.

Fan, J. Q., et al. "Current Advances and Outlooks in Immunotherapy for Pancreatic Ductal Adenocarcinoma." *Mol Cancer* 19.1 (2020): 32. Print.

Farrell, James J, et al. "Human Equilibrative Nucleoside Transporter 1 Levels Predict Response to Gemcitabine in Patients with Pancreatic Cancer." *Gastroenterology* 136.1 (2009): 187-95. Print.

Feig, C., et al. "The Pancreas Cancer Microenvironment." *Clin Cancer Res* 18.16 (2012): 4266-76. Print.

Feig, Christine, et al. "The Pancreas Cancer Microenvironment." *Clinical cancer research : an official journal of the American Association for Cancer Research* 18.16 (2012): 4266-76. Print.

Fisher, David E. "Apoptosis in Cancer Therapy: Crossing the Threshold." *Cell* 78.4 (1994): 539-42. Print.

Fortina, P., et al. "Nanobiotechnology: The Promise and Reality of New Approaches to Molecular Recognition." *Trends Biotechnol* 23.4 (2005): 168-73. Print.

Freelove, Robert, and Anne Walling. "Pancreatic Cancer: Diagnosis and Management." *American family physician* 73.3 (2006): 485-92. Print.

Frese, Kristopher K, et al. "Nab-Paclitaxel Potentiates Gemcitabine Activity by Reducing Cytidine Deaminase Levels in a Mouse Model of Pancreatic Cancer." *Cancer discovery* 2.3 (2012): 260-69. Print.

Fridman, W. H., et al. "The Immune Contexture in Human Tumours: Impact on Clinical Outcome." *Nat Rev Cancer* 12.4 (2012): 298-306. Print.

Grodzinski, P., M. Silver, and L. K. Molnar. "Nanotechnology for Cancer Diagnostics: Promises and Challenges." *Expert Rev Mol Diagn* 6.3 (2006): 307-18. Print.

Haqq, J., et al. "Pancreatic Stellate Cells and Pancreas Cancer: Current Perspectives and Future Strategies." *Eur J Cancer* 50.15 (2014): 2570-82. Print.

He, Lingfeng, et al. "Synergistic Antitumor Effect of Combined Paclitaxel with Fen1 Inhibitor in Cervical Cancer Cells." *DNA repair* 63 (2018): 1-9. Print.

Hezel, A. F., et al. "Genetics and Biology of Pancreatic Ductal Adenocarcinoma." *Genes Dev* 20.10 (2006): 1218-49. Print.

Hosein, P. J., et al. "A Phase Ii Trial of Nab-Paclitaxel as Second-Line Therapy in Patients with Advanced Pancreatic Cancer." *Am J Clin Oncol* 36.2 (2013): 151-6. Print.

Hwang, R. F., et al. "Cancer-Associated Stromal Fibroblasts Promote Pancreatic Tumor Progression." *Cancer Res* 68.3 (2008): 918-26. Print.

Ino, Y., et al. "Immune Cell Infiltration as an Indicator of the Immune Microenvironment of Pancreatic Cancer." *Br J Cancer* 108.4 (2013): 914-23. Print.

Jain, Rakesh K. "Transport of Molecules across Tumor Vasculature." *Cancer and Metastasis Reviews* 6.4 (1987): 559-93. Print.

Jain, T. K., et al. "Iron Oxide Nanoparticles for Sustained Delivery of Anticancer Agents." *Mol Pharm* 2.3 (2005): 194-205. Print.

Jiménez-Guerrero, Rocío, et al. "Obatoclax and Paclitaxel Synergistically Induce Apoptosis and Overcome Paclitaxel Resistance in Urothelial Cancer Cells." *Cancers* 10.12 (2018): 490. Print.

Kamaly, N., et al. "Targeted Polymeric Therapeutic Nanoparticles: Design, Development and Clinical Translation." *Chem Soc Rev* 41.7 (2012): 2971-3010. Print.

Kampan, Nirmala Chandralega, et al. "Paclitaxel and Its Evolving Role in the Management of Ovarian Cancer." *BioMed research international* 2015 (2015). Print.

Karaca, Burcak, et al. "Docetaxel in Combination with Octreotide Shows Synergistic Apoptotic Effect by Increasing Sstr2 and Sstr5 Expression Levels in Prostate and Breast Cancer Cell Lines." *Cancer chemotherapy and pharmacology* 75.6 (2015): 1273-80. Print.

Keane, MG, et al. "A Case–Control Study Comparing the Incidence of Early Symptoms in Pancreatic and Biliary Tract Cancer." *BMJ open* 4.11 (2014): e005720. Print.

Kenmotsu, H., et al. "Phase Ii Study of Nab-Paclitaxel + carboplatin for Patients with Non-Small-Cell Lung Cancer and Interstitial Lung Disease." *Cancer Sci* 110.12 (2019): 3738-45. Print.

Khan, Sheema, et al. "Superparamagnetic Iron Oxide Nanoparticles of Curcumin Enhance Gemcitabine Therapeutic Response in Pancreatic Cancer." *Biomaterials* 208 (2019): 83-97. Print.

Kleeff, J., et al. "Pancreatic Cancer." *Nat Rev Dis Primers* 2 (2016): 16022. Print.

Kleynberg, Roman L, Aijaz A Sofi, and Rekha T Chaudhary. "Hand–Foot Hyperpigmentation Skin Lesions Associated with Combination Gemcitabine–Carboplatin (Gemcarbo) Therapy." *American journal of therapeutics* 18.6 (2011): e261-e63. Print.

Kuwayama, Takashi, et al. "Randomized Multicenter Phase Ii Trial of Neoadjuvant Therapy Comparing Weekly Nab-Paclitaxel Followed by Fec with Docetaxel Followed by Fec in Her2− Early-Stage Breast Cancer." *Clinical breast cancer* 18.6 (2018): 474-80. Print.

Le, D. T., et al. "Evaluation of Ipilimumab in Combination with Allogeneic Pancreatic Tumor Cells Transfected with a Gm-Csf Gene in Previously Treated Pancreatic Cancer." *J Immunother* 36.7 (2013): 382-9. Print.

Le, Dung T, et al. "Evaluation of Ipilimumab in Combination with Allogeneic Pancreatic Tumor Cells Transfected with a Gm-Csf Gene in Previously Treated Pancreatic Cancer." *Journal of immunotherapy (Hagerstown, Md.: 1997)* 36.7 (2013): 382. Print.

Li, Chunxiao, et al. "Tumor-Associated Macrophages: Potential Therapeutic Strategies and Future Prospects in Cancer." *Journal for ImmunoTherapy of Cancer* 9.1 (2021). Print.

Lindquist, C. M., et al. "Pancreatic Cancer Screening." *Abdom Radiol (NY)* 43.2 (2018): 264-72. Print.

Lonardo, E., et al. "Pancreatic Stellate Cells Form a Niche for Cancer Stem Cells and Promote Their Self-Renewal and Invasiveness." *Cell Cycle* 11.7 (2012): 1282-90. Print.

Lowenfels, Albert B., et al. "Pancreatitis and the Risk of Pancreatic Cancer." *New England Journal of Medicine* 328.20 (1993): 1433-37. Print.

Maeda, Shimpei, et al. "Paclitaxel as Second-Line Chemotherapy in Patients with Gemcitabine-Refractory Pancreatic Cancer: A Retrospective Study." *International journal of clinical oncology* 16.5 (2011): 539-45. Print.

Markman, Janet L, et al. "Nanomedicine Therapeutic Approaches to Overcome Cancer Drug Resistance." *Advanced drug delivery reviews* 65.13-14 (2013): 1866-79. Print.

Massey, Andrew E, et al. "Next-Generation Paclitaxel-Nanoparticle Formulation for Pancreatic Cancer Treatment." *Nanomedicine: Nanotechnology, Biology and Medicine* 20 (2019): 102027. Print.

Meng, Z., et al. "Prodrug Strategies for Paclitaxel." *Int J Mol Sci* 17.5 (2016). Print.

Mohammed, A., et al. "Targeting Pancreatitis Blocks Tumor-Initiating Stem Cells and Pancreatic Cancer Progression." *Oncotarget* 6.17 (2015): 15524-39. Print.

Neesse, A., et al. "Stromal Biology and Therapy in Pancreatic Cancer: A Changing Paradigm." *Gut* 64.9 (2015): 1476-84. Print.

Neesse, Albrecht, et al. "Stromal Biology and Therapy in Pancreatic Cancer." *Gut* 60.6 (2011): 861-68. Print.

Network, Pancreatic Cancer Action. "What Is Pancreatic Cancer?" 2022. Web. 05-16-2022 2022.

---. "What Is the Pancreas?" 2022. Web. 05-16-2022 2022.

Palacio, Sofia, et al. "The Nab-Paclitaxel/Gemcitabine Regimen for Patients with Refractory Advanced Pancreatic Adenocarcinoma." *Journal of gastrointestinal oncology* 9.1 (2018): 135. Print.

Pan, B., et al. "Cancer-Associated Fibroblasts in Pancreatic Adenocarcinoma." *Future Oncol* 11.18 (2015): 2603-10. Print.

Pandha, H., et al. "Loss of Expression of Antigen-Presenting Molecules in Human Pancreatic Cancer and Pancreatic Cancer Cell Lines." *Clin Exp Immunol* 148.1 (2007): 127-35. Print.

Parisi, A., et al. "First-Line Carboplatin/Nab-Paclitaxel in Advanced Ovarian Cancer Patients, after Hypersensitivity Reaction to Solvent-Based Taxanes: A Single-Institution Experience." *Clin Transl Oncol* 22.1 (2020): 158-62. Print.

Park, Hyung, Wooram Park, and Kun Na. "Doxorubicin Loaded Singlet-Oxygen Producible Polymeric Micelle Based on Chlorine E6 Conjugated Pluronic F127 for Overcoming Drug Resistance in Cancer." *Biomaterials* 35.27 (2014): 7963-69. Print.

Park, J. W., et al. "Immunoliposomes for Cancer Treatment." *Adv Pharmacol* 40 (1997): 399-435. Print.

Phase I Studies of Gemcitabine Combined with Carboplatin or Paclitaxel. Seminars in oncology. 1997. Print.

Pedziwiatr-Werbicka, Elzbieta, et al. "Nanoparticles in Combating Cancer: Opportunities and Limitations: A Brief Review." *Current Medicinal Chemistry* 28.2 (2021): 346-59. Print.

Pelosi, E., G. Castelli, and U. Testa. "Pancreatic Cancer: Molecular Characterization, Clonal Evolution and Cancer Stem Cells." *Biomedicines* 5.4 (2017). Print.

Peng, Y. P., et al. "Elevation of Mmp-9 and Ido Induced by Pancreatic Cancer Cells Mediates Natural Killer Cell Dysfunction." *BMC Cancer* 14 (2014): 738. Print.

Perez, Edith A. "Paclitaxel in Breast Cancer." *The oncologist* 3.6 (1998): 373-89. Print.

Polireddy, K., and Q. Chen. "Cancer of the Pancreas: Molecular Pathways and Current Advancement in Treatment." *J Cancer* 7.11 (2016): 1497-514. Print.

Pries, Axel R, et al. "The Shunt Problem: Control of Functional Shunting in Normal and Tumour Vasculature." *Nature Reviews Cancer* 10.8 (2010): 587-93. Print.

Protti, M. P., and L. De Monte. "Immune Infiltrates as Predictive Markers of Survival in Pancreatic Cancer Patients." *Front Physiol* 4 (2013): 210. Print.

Provenzano, Paolo P, et al. "Enzymatic Targeting of the Stroma Ablates Physical Barriers to Treatment of Pancreatic Ductal Adenocarcinoma." *Cancer cell* 21.3 (2012): 418-29. Print.

Ramalingam, Sakkaraiappan, and Chandra P Belani. "Paclitaxel for Non-Small Cell Lung Cancer." *Expert opinion on pharmacotherapy* 5.8 (2004): 1771-80. Print.

Rapoport, Natalya, et al. "Ultrasonic Nanotherapy of Pancreatic Cancer: Lessons from Ultrasound Imaging." *Molecular pharmaceutics* 7.1 (2010): 22-31. Print.

Rawla, Prashanth, Tagore Sunkara, and Vinaya Gaduputi. "Epidemiology of Pancreatic Cancer: Global Trends, Etiology and Risk Factors." *World journal of oncology* 10.1 (2019): 10. Print.

Ryschich, E., et al. "Control of T-Cell-Mediated Immune Response by Hla Class I in Human Pancreatic Carcinoma." *Clin Cancer Res* 11.2 Pt 1 (2005): 498-504. Print.

Sahoo, S. K., and V. Labhasetwar. "Nanotech Approaches to Drug Delivery and Imaging." *Drug Discov Today* 8.24 (2003): 1112-20. Print.

Sanford, D. E., et al. "Inflammatory Monocyte Mobilization Decreases Patient Survival in Pancreatic Cancer: A Role for Targeting the Ccl2/Ccr2 Axis." *Clin Cancer Res* 19.13 (2013): 3404-15. Print.

Sapra, P., and T. M. Allen. "Ligand-Targeted Liposomal Anticancer Drugs." *Prog Lipid Res* 42.5 (2003): 439-62. Print.

Schizas, Dimitrios, et al. "Immunotherapy for Pancreatic Cancer: A 2020 Update." *Cancer treatment reviews* 86 (2020): 102016. Print.

Schmid, P., et al. "Atezolizumab and Nab-Paclitaxel in Advanced Triple-Negative Breast Cancer." *N Engl J Med* 379.22 (2018): 2108-21. Print.

Sclafani, Francesco, et al. "Management of Metastatic Pancreatic Cancer: Current Treatment Options and Potential New Therapeutic Targets." *Critical reviews in oncology/hematology* 95.3 (2015): 318-36. Print.

Sengupta, S., et al. "Temporal Targeting of Tumour Cells and Neovasculature with a Nanoscale Delivery System." *Nature* 436.7050 (2005): 568-72. Print.

Shepard, D. R., et al. "Phase Ii Trial of Neoadjuvant Nab-Paclitaxel in High Risk Patients with Prostate Cancer Undergoing Radical Prostatectomy." *J Urol* 181.4 (2009): 1672-7; discussion 77. Print.

Shetty, Advait, et al. "Novel Paclitaxel Nanoformulation Impairs De Novo Lipid Synthesis in Pancreatic Cancer Cells and Enhances Gemcitabine Efficacy." *ACS omega* 5.15 (2020): 8982-91. Print.

Shi, C., et al. "Fibrogenesis in Pancreatic Cancer Is a Dynamic Process Regulated by Macrophage-Stellate Cell Interaction." *Lab Invest* 94.4 (2014): 409-21. Print.

Siegel, Rebecca, D Naishadham, and A Jemal. "Global Cancer Statistics." *CA Cancer J Clin* 63.1 (2013): 11-30. Print.

Siegel RL, Miller KD, Jemal A. . " Cancer Statistics." (2020). Print.

Simoes, P. K., et al. "Epidemiology of Pancreatic Adenocarcinoma." *Chin Clin Oncol* 6.3 (2017): 24. Print.

Sosnik, Alejandro. "Reversal of Multidrug Resistance by the Inhibition of Atp-Binding Cassette Pumps Employing “Generally Recognized as Safe”(Gras) Nanopharmaceuticals: A Review." *Advanced drug delivery reviews* 65.13-14 (2013): 1828-51. Print.

Sperb, Nadine, Miltiadis Tsesmelis, and Thomas Wirth. "Crosstalk between Tumor and Stromal Cells in Pancreatic Ductal Adenocarcinoma." *International journal of molecular sciences* 21.15 (2020): 5486. Print.

Stathis, Anastasios, and Malcolm J Moore. "Advanced Pancreatic Carcinoma: Current Treatment and Future Challenges." *Nature reviews Clinical oncology* 7.3 (2010): 163-72. Print.

Stylianopoulos, T., et al. "Multistage Nanoparticles for Improved Delivery into Tumor Tissue." *Methods Enzymol* 508 (2012): 109-30. Print.

Stylianopoulos, Triantafyllos, et al. "Causes, Consequences, and Remedies for Growth-Induced Solid Stress in Murine and Human Tumors." *Proceedings of the National Academy of Sciences* 109.38 (2012): 15101-08. Print.

Sung, Hyuna, et al. "Global Cancer Statistics 2020: Globocan Estimates of Incidence and Mortality Worldwide for 36 Cancers in 185 Countries." *CA: a cancer journal for clinicians* 71.3 (2021): 209-49. Print.

Tan, M. C., et al. "Disruption of Ccr5-Dependent Homing of Regulatory T Cells Inhibits Tumor Growth in a Murine Model of Pancreatic Cancer." *J Immunol* 182.3 (2009): 1746-55. Print.

Tang, D., et al. "Apoptosis and Anergy of T Cell Induced by Pancreatic Stellate Cells-Derived Galectin-1 in Pancreatic Cancer." *Tumour Biol* 36.7 (2015): 5617-26. Print.

Tesfaye, A. A., et al. "The Evolution into Personalized Therapies in Pancreatic Ductal Adenocarcinoma: Challenges and Opportunities." *Expert Rev Anticancer Ther* 18.2 (2018): 131-48. Print.

Tesfaye, Anteneh A, et al. "The Evolution into Personalized Therapies in Pancreatic Ductal Adenocarcinoma: Challenges and Opportunities." *Expert review of anticancer therapy* 18.2 (2018): 131-48. Print.

Torphy, R. J., Y. Zhu, and R. D. Schulick. "Immunotherapy for Pancreatic Cancer: Barriers and Breakthroughs." *Ann Gastroenterol Surg* 2.4 (2018): 274-81. Print.

Ushio, J., et al. "Pancreatic Ductal Adenocarcinoma: Epidemiology and Risk Factors." *Diagnostics (Basel)* 11.3 (2021). Print.

Uyttenhove, C., et al. "Evidence for a Tumoral Immune Resistance Mechanism Based on Tryptophan Degradation by Indoleamine 2,3-Dioxygenase." *Nat Med* 9.10 (2003): 1269-74. Print.

Vasir, J. K., and V. Labhasetwar. "Polymeric Nanoparticles for Gene Delivery." *Expert Opin Drug Deliv* 3.3 (2006): 325-44. Print.

---. "Targeted Drug Delivery in Cancer Therapy." *Technol Cancer Res Treat* 4.4 (2005): 363-74. Print.

von Bernstorff, W., et al. "Pancreatic Cancer Cells Can Evade Immune Surveillance Via Nonfunctional Fas (Apo-1/Cd95) Receptors and Aberrant Expression of Functional Fas Ligand." *Surgery* 125.1 (1999): 73-84. Print.

Von, DD Hoff, et al. "Increased Survival in Pancreatic Cancer with Nab-Paclitaxel Plus Gemcitabine." *The New England journal of medicine* 369.18 (2013): 1691-703. Print.

Von Hoff, D. D., et al. "Gemcitabine Plus Nab-Paclitaxel Is an Active Regimen in Patients with Advanced Pancreatic Cancer: A Phase I/Ii Trial." *J Clin Oncol* 29.34 (2011): 4548-54. Print.

Wang, Jiawei, et al. "Drug-Free Macromolecular Therapeutics Induce Apoptosis in Cells Isolated from Patients with B Cell Malignancies with Enhanced Apoptosis Induction by Pretreatment with Gemcitabine." *Nanomedicine: Nanotechnology, Biology and Medicine* 16 (2019): 217-25. Print.

Wang, X., et al. "Cancer-Foxp3 Directly Activated Ccl5 to Recruit Foxp3(+)Treg Cells in Pancreatic Ductal Adenocarcinoma." *Oncogene* 36.21 (2017): 3048-58. Print.

Weinberg, RA, and Douglas Hanahan. "The Hallmarks of Cancer." *Cell* 100.1 (2000): 57-70. Print.

Wörmann, S. M., et al. "The Immune Network in Pancreatic Cancer Development and Progression." *Oncogene* 33.23 (2014): 2956-67. Print.

Xu, Q., et al. "Stromal-Derived Factor-1alpha/Cxcl12-Cxcr4 Chemotactic Pathway Promotes Perineural Invasion in Pancreatic Cancer." *Oncotarget* 6.7 (2015): 4717-32. Print.

Yallapu, Murali M, et al. "Anti-Cancer Activity of Curcumin Loaded Nanoparticles in Prostate Cancer." *Biomaterials* 35.30 (2014): 8635-48. Print.

Yallapu, Murali Mohan, et al. "Fabrication of Curcumin Encapsulated Plga Nanoparticles for Improved Therapeutic Effects in Metastatic Cancer Cells." *Journal of colloid and interface science* 351.1 (2010): 19-29. Print.

Yallapu, Murali Mohan, Meena Jaggi, and Subhash C Chauhan. "Poly (B-Cyclodextrin)/Curcumin Self-Assembly: A Novel Approach to Improve Curcumin Delivery and Its Therapeutic Efficacy in Prostate Cancer Cells." *Macromolecular bioscience* 10.10 (2010): 1141-51. Print.

Yeo, T. P. "Demographics, Epidemiology, and Inheritance of Pancreatic Ductal Adenocarcinoma." *Semin Oncol* 42.1 (2015): 8-18. Print.

Yoshikawa, K., et al. "Impact of Tumor-Associated Macrophages on Invasive Ductal Carcinoma of the Pancreas Head." *Cancer Sci* 103.11 (2012): 2012-20. Print.

Zhang, L., et al. "Nanoparticles in Medicine: Therapeutic Applications and Developments." *Clin Pharmacol Ther* 83.5 (2008): 761-9. Print.

Zhang, Lulu, Santosh Sanagapalli, and Alina Stoita. "Challenges in Diagnosis of Pancreatic Cancer." *World journal of gastroenterology* 24.19 (2018): 2047. Print.

Zhang, Wei, et al. "Multifunctional Pluronic P123/F127 Mixed Polymeric Micelles Loaded with Paclitaxel for the Treatment of Multidrug Resistant Tumors." *Biomaterials* 32.11 (2011): 2894-906. Print.

Zheng, L., et al. "Role of Immune Cells and Immune-Based Therapies in Pancreatitis and Pancreatic Ductal Adenocarcinoma." *Gastroenterology* 144.6 (2013): 1230-40. Print.

BIOGRAPHICAL SKETCH

Godwin Peasah-Darkwah was a Graduate Research Assistant in the Department of Immunology and Microbiology at the School of Medicine, University of Texas Rio Grande Valley in Edinburg, TX. He previously earned his bachelor's degree in Biological Sciences at the Kwame Nkrumah University of Science and Technology in Ghana in June 2019 and gained admission to pursue his master's degree in Biochemistry and Molecular Biology at the University of Texas Rio Grande Valley in January 2021. He earned his master's degree at the University of Texas Rio Grande Valley in July 2022 and his research centered on drug discovery and development for PanCa therapy. His dedicated effort towards bridging global cancer health disparities was his driving motive throughout his years of research as he sought to churn out ingenuine ideas and creative solutions for cancer therapy, and that is still his goal. His personal email is: godwinpeasahdarkwah@gmail.com.